research articles Journal of proteome research

Identification of Protein Clusters Predictive of Response to Chemotherapy in Breast Cancer Patients

Laura Cortesi,[†] Andrea Barchetti,[||] Elisabetta De Matteis,[†] Elena Rossi,[||] Lara Della Casa,[||] Luigi Marcheselli,[†] Giovanni Tazzioli,[‡] Maria Grazia Lazzaretti,[⊥] Guido Ficarra,[§] Massimo Federico,[†] and Anna Iannone*,[||]

Department of Oncology & Haematology, Department of General Surgery and Surgical Specialties, Department of Laboratory, Pathological Anatomy and Forensic Medicine, and "ProteoWork Lab" of the Department of Biomedical Sciences, University of Modena and Reggio Emilia, Modena, and General Surgery Unit, "Ramazzini" Hospital, Carpi (Modena), Italy

Received March 11, 2009

An attempt for the identification of potential biomarkers predictive of response to chemotherapy (CHT) in breast cancer patients has been performed by the use of two-dimensional electrophoresis and mass spectrometry analysis. Since growth and progression of tumor cells depend also on stromal factors in the microenvironment, we choose to investigate the proteins secreted in Tumor Interstitial Fluid (TIF) and in Normal Interstitial Fluids (NIF). One-hundred and twenty-two proteins have been analyzed and a comparison was also made between the proteomic profile of responders versus nonresponders to CHT. At baseline, proteins isolated in TIF and NIF of all the 28 patients show significant differences in expression. Two clusters of proteins, differentially expressed in TIF with respect to NIF were found. Most significant is the decreased expression in TIF of CRYAB. In the protein metabolism group, also FIBB was found decreased. Some proteins involved in energy pathways were overexpressed (PGAM-1, ALDO A, PGK1, G3Pcn), while some other were down-regulated (CAH2, G3Pdx, PRDX6, TPIS). The same trend was observed for signal transduction proteins, with 14−3−3-Z overexpressed, and ANXA2 and PEBP 1 down-regulated. Moreover, an analysis has been conducted comparing protein expression in interstitial fluids of responders and nonresponders, irrespective of TIF or NIF source. This analysis lead us to identify two clusters of proteins with a modified expression, which might be predictive of response to CHT. In responders, an increase in expression of LDHA, G3Pdx, PGK1sx (energy pathways), VIME (cell growth and maintenance) and 14−3−3-Z (signal transduction), coupled with a decreased expression of TPIS, CAH 2, G3Psx, PGK 1dx (energy pathways), TBB5 (cell growth and maintenance), LDHB and FIBB (protein metabolism), was found. We observed that CHT modifies the expression of these cluster proteins since, after treatment, their expression in TIF of responder is generally decreased. Patients not responding to CHT show an unchanged expression pattern in TIF, with the exception of protein 14−3−3-Z, which is overexpressed, and a decreased expression in NIF of several cluster proteins. In conclusion, the identification of protein clusters associated with response to CHT might be important for predicting the efficacy of a specific antineoplastic drug and for the development of less empiric strategies in choosing the therapy to be prescribed to the single patient.

Keywords: Breast cancer • chemotherapy • biomarkers • tumor interstitial fluid

Introduction

Breast cancer is the most frequent cancer affecting women in Western countries. Accumulation of several, and often unknown, molecular alterations is responsible for cell proliferation, genetic instability and acquisition of an increasingly invasive and resistant phenotype. Survival of patients has increased over the last decades in relation to earlier diagnosis and more effective systemic therapies (hormonal therapy and chemotherapy). However, the efficacy of combination chemotherapies is variable, and we do not know yet the underlying mechanisms. In an attempt to improve the ability in choosing the more appropriate antineoplastic drugs, we investigated the proteomic profile of patients responding or not to the chemo-

* To whom correspondence should be addressed. Anna Iannone, "ProteoWork Lab" of the Department of Biomedical Sciences, via Campi 287, 41125 Modena, Italy. Tel., ++39.059.2055420; fax, + +39.059.2055426; e-mail, anna.iannone@unimore.it.

[†] Department of Oncology & Haematology, University of Modena and Reggio Emilia.

[||] "ProteoWork Lab" of the Department of Biomedical Sciences, University of Modena and Reggio Emilia.

[‡] Department of General Surgery and Surgical Specialties, University of Modena and Reggio Emilia.

[⊥] "Ramazzini" Hospital.

[§] Department of Laboratory, Pathological Anatomy and Forensic Medicine, University of Modena and Reggio Emilia.

Published on Web 09/09/2009

10.1021/pr900239h CCC: $40.75
© 2009 American Chemical Society

therapeutic agents epirubicin and docetaxel. This approach is justified since, while some mechanisms of mammary oncogenesis have been elucidated and key genes identified, the heterogeneity of malignant cells and the variability of the host background highlight molecularly distinct subgroups which lead to different phenotypes and clinical outcomes. Moreover, this heterogeneity is only partially apprehended by the clinical and pathological parameters currently used by clinicians, and this perplexes diagnosis and therapy for each case. Proteomics has the potential to complement and further enlarge the wealth of information generated by genomics, because mRNA levels do not necessarily correlate with corresponding protein abundance.[1−5] Additional complexity is conferred by protein post-translational modifications, including phosphorylation, acetylation, glycosylation, and protein cleavage.[6] These modifications are not detectable at the mRNA level; however, they play significant roles in protein stability, localization, interactions, and functions. Moreover, proteins represent more accessible and relevant therapeutic targets than nucleic acids. Several proteomic studies have compared normal and cancerous breast cells.[7] A hierarchical clustering analysis of proteomes of normal and different stages of disease has shown that it is possible to distinguish between normal, benign, and cancerous breast tissues on the basis of the protein profile.[8] Interestingly, many proteins that have been identified by proteomic studies are different from those found by nucleic acid-based studies. During the last years, there have been numerous reports indicating that growth and progression of breast, as well as other tumor cells, depend not only on their malignant potential, but also on stromal factors present in the tumor microenvironment, the insoluble extra cellular matrix, as well as cell−cell interactions.[9−14] The microenvironment is considered an active contributor to tumor spreading, with the possibility of controlling the course of breast cancer progression: it has been recently demonstrated that changes in gene expression profiling of the tumor microenvironment occur during breast cancer progression from normal to preinvasive to invasive ductal carcinoma, and that tumor microenvironment participates in tumorigenesis even before tumor cells invade into stroma.[15] Recently, also the tumor microenvironment of metastasis in breast cancer patients has been studied with the aim to predict the development of metastases.[16]

Protein composition of the microenvironment might well reflects the physiological and pathological state of the breast tissue and could provide a new and potentially rich resource for diagnostic biomarker discovery and for identifying more selective targets for therapeutic intervention. Moreover, the study of the breast interstitial fluids clinical specimens, with or without pharmacologic intervention, will stand to assist in bridging the gap between respective tissue and serum samples and will contribute in the discovery of drug efficacy markers.

Celis and colleagues have already used this approach[17,18] and characterized proteins released in the interstitial space by the cells resident in the tumor microenvironment. They studied the protein composition of the nipple aspirate fluid and of tumor interstitial fluids in patients with breast cancer: several proteins have been identified in the microenvironment, and they might be responsible for the biological modification of the neoplastic cell.

However, the identity of many proteins still remain to be determined. On this basis, we chose to investigate the proteins secreted in Tumor Interstitial Fluid (TIF) and in Normal Interstitial Fluids (NIF) of breast cancer patients in the search of a combination of biomarkers that will probably be more sensitive and specific than a single molecular marker for screening, diagnosis, prognosis, and prediction of therapeutic response. This is of peculiar relevance since until now the FDA (Food and Drug Administration) has not approved any cancer-related biomarker assay that uses new genomics or proteomic technologies, with the exception of a UGT1A1 genetic assay, which is a biomarker for predicting colon cancer in patients at risk for the toxic effect of the irinotecan. In this study, we characterized 122 proteins by cLC-nESI QqTOF MS; subsequently, a comparison was made between the proteome of patients responders to chemotherapy versus nonresponders, with the aim to identify potential predictive biomarkers of chemotherapy response. The main challenge, however, remains the application of these technologies to clinically relevant samples in a well-defined clinical and pathological framework to suit the FDA biomarker guidelines.[19]

Experimental Procedures

Recruitment of Patients. Thirty-seven patients (age 17−86) were recruited from the Department of Onco-Haematology of the University Hospital of Modena, Italy. They had no previous surgery to the breast and did not receive preoperative treatment. Written informed consent was obtained from all recruited subjects. We collected breast tissue samples during vacuum assisted biopsy exam or surgery: 23 were ductal carcinoma, 5 lobular carcinoma, and 9 benign disease. The latter, after the histological analysis, where not further processed. Twelve patients with ductal carcinoma and 2 patients with the lobular histotype were treated with 4 courses of FEC90 every 3 weeks (F, fluorouracil 500 mg/mq; E, epirubicin 90 mg/mq; C, cyclophosphamide 500 mg/mq) followed by 4 cycles of docetaxel (T) 100 mg/mq every 3 weeks. Ultrasound and mammographic exam were performed before and after the treatment to evaluate the tumor size. Finally, surgery was performed and further samples were collected at this time. All tumor samples were histological grade 2 and 3 with dimensions more than 10 mm; for each patient, we collected at least 200 mg of tumor and normal tissue.

Reagents. Thirty percent Acrylamide/bis (Cat. No. 161−0156), ampholines (Bio Lyte ampholyte pH 3−10, Cat. No. 163−1112), Protein Assay Dye Reagent Concentrate (Cat. No. 500−0006), DTT, Cat. No. 161−0611, iodoacetamide (Cat. No. 161−2109), mineral oil (Cat. No. 163-2129), *N,N,N,N′N′*-tetramethylenediamine (TEMED, Cat. No. 161−0801), overlay agarose 0.5% (Cat. No. 163-2111), ready strip (IPG strips 17 cm pH3−10NL Cat. No. 163−2009) and urea (Cat. No. 161−0731), tris/glycine/SDS (TGS) as running buffer 10×, pH 8.3 (Cat. No. 161−0772) were obtained from Bio-Rad. Ammonium persulfate (Cat. No. A3678), ammonium bicarbonate (Cat. No. A6141), bromophenol blue (BPB; Cat. No. B-6131), calcium chloride dihydrate (Cat. No. C5080), CHAPS (Cat. No. C9426), formaldehyde (Cat. No. F8775), glycerol (Cat. No. G8773), potassium carbonate (Cat. No. P5833), potassium hexacyanoferrate III (Cat. No. P8131), potassium tetrathionate (Cat. No. P2926), silver nitrate (Cat. No. S8157), sodium thiosulfate (Cat. No. S7026), thiourea (Cat. No. T8656), tributylphosphate (Cat. No. 158615) and tris (Cat. No. 15456−3) were purchased from Sigma. Acetone (Cat. No. 8142), acetic acid (Cat. No. 6152), ethanol (Cat. No. 8462) and methanol (Cat. No. 8402) were purchased from J.T.Baker. Trypsin gold (Mass Spectrometry grade, Cat. No. V5280) was purchased from Promega. Potassium acetate (Cat. No. 60035) and SDS (Cat. No. 05030) were purchased from Fluka.

TIF and NIF Collection. Breast tissue samples from vacuum-assisted biopsy or surgery were collected from the University Hospital of Modena and from the "Ramazzini" Hospital in Carpi (Modena), placed in ice and rapidly delivered to the "ProteoWork" laboratory of the Department of Biomedical Sciences, for processing. Within 1 h from the collection, about 200 mg of clean tissue was cut into small pieces (3 × 3 mm), washed carefully in 5 mL of PBS, and placed in a 15-mL conical plastic tube, containing 0.8 mL of PBS. Samples were then incubated at 37 °C in a humidified CO_2 incubator. After 1-h incubation, samples underwent to a two-step centrifugation: 1000*g* for 1 min, with the subsequent recovery of the supernatant, followed by a further centrifugation at 2000*g* for 5 min for recovering the residual supernatant. Immediately after, 14 vol of precipitation mix (12 vol of acetone, 1 vol of methanol, 1 vol of tributylphosphate) was added to the supernatant and incubated at −20 °C overnight. The following day, samples were centrifuged for 1 min at 2000*g*; the pellets were air-dried and resuspended in rehydratation buffer (6 M urea, 2 M thiourea, 4% CHAPS, 25 mM DTT, 0.2% ampholine 40%). Samples concentration was estimated by Protein Assay Dye Reagent Concentrate (Bio-Rad): 80 μg aliquots were stored at −80 °C.

First Dimension. A total of 80 μg of proteins in rehydratation buffer with a final volume of 300 μL and trace of BPB were used for each IPG strips (17 cm pH 3−10 NL). After 12 h of active rehydratation performed in Protean IEF Cell from Bio-Rad (50 V and 20 °C), the isoelectric focusing was carried out by rapidly increasing voltage until 250 V for 15 min, then linearly increasing voltage from 250 to 10 000 V for the next 3 h; after that, focusing was continued at 10 000 V until 60 000 total Vh. Once IEF was finished, strips were either stored at −80 °C for further use, or equilibrated and loaded in the second dimension.

Equilibration. IPG strips were shaken in glass tubes at room temperature (RT) for 15 min in equilibration buffer (urea, 50 mM tris, pH 8.8, 30% glycerol, 2% SDS, trace of BPB) with 1% DTT to reduce disulphuric bonds. The -SH groups were then blocked by substituting the DTT with 2.5% iodoacetamide in equilibration buffer and shaking in glass tubes for 15 min at RT. The strips were soaked in running buffer just before the second dimension.

Two-Dimensional Gel Electrophoresis. Strips were applied on 10% polyacrylamide (30% acrylamide-bis, 3.3 mL; 1.5 M tris pH 8.8, 2.5 mL; 10% SDS, 0.1 mL; 10% APS, 0.1 mL; TEMED 0.004 mL; water, 4 mL) 20 cm gels (SDS-PAGE) with hot overlay agarose 0.5%. The electrophoresis was performed in PROTEAN II xi 2-D cell (Bio-Rad), filled with running buffer (TGS 1× pH 8.3: 250 mM Tris, 1.92 M glycine, 1% SDS). The run was carried out with a constant current of 40 mA/gel for 30 min, followed by constant 500 V at 10 °C.

Silver Staining. All the staining procedures were performed at room temperature, with ultrapure water (Millipore water system), using an orbital shaker (IKA-KS260). After electrophoresis, the gel slab was fixed in 30% ethanol, 10% acetic acid (4 times for 30 min). It was then washed 2 times for 20 min with 30% ethanol. To remove the remaining acid, the gel was washed overnight with water. The gel was sensitized for 45 min with the Enhancer solution (30% ethanol, 0.3% K-tetrathionate, 0.5 M K-acetate); then it was rinsed with water 6 times for 5 min. The gel was stained in the dark with 0.2% silver nitrate for 75 min. The silver nitrate was then discarded and the gel slab rinsed with water for 1 min. It was incubated with developer solution (3% K-carbonate, 0.03% formaldehyde, 0.03% Na-thiosulphate) for up to 45 min, until the desired intensity was reached: the process was stopped by removing the developer and adding the blocking solution (4% tris, 2% acetic acid) for 30 min. Two more steps of washing with water for 15 min were performed before storing the gel in 1% acetic acid at 4 °C.

Imaging Capture and Analysis. All stained gels images were captured with Epson Perfection V10 and then analyzed with PD-Quest Software from Bio-Rad. All interesting spots resulted from bioinformatics analysis have been processed and sent to the mass spectrometry core for identification.

In-Gel Digestion. Protein spots were excised from the gel with a sterile plastic pipet and in-gel digested with trypsin in 0.5 mL polypropylene tubes. A piece of gel was cut from albumin region as control and processed in parallel with the samples. Gel pieces were incubated with 150 μL of destaining solution (100 mM Na-thiosulfate, 30 mM potassium hexacyanoferrate III) and mixed for 20 min in the dark at RT. The solution was removed and a two-step wash with 100 μL of water and shaking for 10 min at RT was performed. Gel pieces were subjected to two-step dehydratation with 100 μL of acetonitrile (ACN) and shaking for 5 s; ACN was then removed, the gel was shrunk, and white gel pieces were obtained. Proteins were then subjected to reduction and alkylation. The gel pieces were incubated with 50 μL of 10 mM DTT, in 50 mM ammonium bicarbonate (AmBic) and shaken for 30 min at 56 °C; the solution was removed, 50 μL of 55 mM iodoacetamide (in 50 mM AmBic) was added, and the solution was shaken for 20 min at RT and in the dark. The solution was removed and gel pieces were dried in Savant Speed-Vac System for 15−20 min. Proteins were then digested with 30 μL of trypsin solution (for each spot: 300 ng of trypsin, 10 μL of 50 mM AmBic, 1 μL of 120 mM $CaCl_2 \cdot 2H_2O$ and water up to 24 μL) on ice for 30 min; the solution was removed and 30 μL of Incubation solution (for each spot: 10 μL of 50 mM AmBic, 1 μL of 120 mM $CaCl_2 \cdot 2H_2O$ and water up to 24 μL) was added. These samples were shacked overnight at 37 °C.

The next day, supernatant from each tube was collected and the gel pieces were added with 15 μL of 25 mM AmBic and 15 μL ACN: each step was followed by 15 min of mixing at 37 °C. The supernatant was collected and the gel pieces were added with 50 μL of 5% formic acid and 15 μL of ACN: each step was followed by 15 min of mixing at 37 °C. The final supernatant was collected and added to the previous for each spot and dried in Speed Vac for 2 h. Samples were stored in −80 °C until MASS SPEC analysis.

Capillary High-Performance Liquid Chromatography (Capillary LC). Nano electrospray experiments were conducted on a Q-TOF Ultima Global (MICROMASS) equipped with a nano electrospray Z spray source and coupled with HPLC CapLC (Waters). The instrument was operated in the V mode to achieve a mass resolution of 8−10 000.

Dried peptide mixtures from the trypsin digest were resuspended in 5% formic acid to a final concentration of 1 pM/μL; a binary gradient was generated using the binary pump. Peptides were eluted from the trap column with increasing organic phase (ACN), refocused, and separated on a Waters Nano Ease Atlantis dC18 nano column (75 μm i.d., 150 mm length, 3 μm particle size, 100 Å porosity). The peptides were eluted using an elution gradient with buffer A (Milli-Q water/ACN/formic acid, 97.9/2/0.1) and B (Milli-Q water/ACN/formic acid, 4.9/95/0.1). HPLC program was 95% buffer A and 5% buffer B for the first 3 min. After, buffer B was increased to

28% in 24 min, then to 85% in 6 min and maintained constant for 3 min. Finally, buffer B was decreased to 5% and kept constant until the end of the run. During the run, flow was always 5 μL/min. Samples were transported inside the column by an auxiliary solution, with buffer A. Flow was 30 μL/min for the first 3 min, during which samples were carried on the precolumn (Dionex, 5 mm $\times$ 300 μm i.d., packed with C18 PepMap100). After that, flow was decreased to 1 μL/min for all the remaining time. All solvents were HPLC grade.

Databank Search and Sequence Analysis. The MASCOT MS/MS ion search program (www.matrixscience.com) was used for peptide sequence searching. Some restrictions were selected for searching the SWISS-PROT database: species, *Homo sapiens* (Human); one missed trypsin cleavage; peptide tolerance $\pm$0.8 Da; and a MS/MS tolerance error of $\pm$0.4 Da. The mowse score cutoff for 95% protein identification was set to 37. Moreover, search parameters allowed for carbamidomethylation of cysteine in fixed modifications.

The highest score hits among MASCOT search results were selected. The Micromass software (MassLynx) allows for the automated selection of peptides for fragmentation (and therefore primary structure determination) when peptide ions above a certain detection level are recorded. Since ESI normally produces multiply charged peptide ions, parameters were chosen so that only multiply charged ions were selected for sequencing by MS/MS.

Immunohistochemistry. The immunohistochemical analysis was performed to evaluate the receptor status and the amplification status of c-ERB gene. Tumour specimens were fixed in 10% neutral-buffered formalin for 20−28 h before processing and embedding in paraffin wax blocks.

The antibodies used were Estrogen Receptor clone 6F11, Ventana; Progesterone Receptor clone 1E2, Ventana; HER2/neu clone CB11, Novocastra, diluted at 1:120; Ki 67 clone mib-1 diluted at 1:200.

Immunohistochemical staining was performed according to the avidin−biotin method, using tissue sections of 3 μm thickness. After deparaffinization in xylene and graded alcohols, epitope retrieval was performed. Antigene retrieval was made in 10 mM EDTA buffer (pH 8) in microwave.

Subsequently, endogenous peroxidase was blocked by 0.3% hydrogen peroxide for 15 min. Sections were incubated with primary antibody for 30 min at 37 °C, then with the biotinylated secondary antibody for 20 min at 37 °C and then in avidin−biotin complex for a further 45 min. Diaminobenzidine tetrahydrochloride (DAB) was used as chromogen. Immunohistochemical staining was performed on Ventana Benchmark autostainer.

The scoring for HER2 results assessed by immunohistochemistry has been divided into the following categories: samples with no membrane staining are scored 0, samples with a partial membrane staining in more than 10% of tumor cells are scored 1+; samples with weak complete staining in more than 10% of tumor cells are scored 2+; samples showing intense complete staining of the membrane in more than 10% of tumor cells are scored 3+.

Fluorescence in situ hybridization (FISH) analysis was performed only in the four cases scored as 2+. It has been performed using the PathVysion (Vysis, Inc., Downers Grove, IL).

ER and PGR receptor status has been tested by evaluating the percentage (%) of nuclear immunoreactivity with respect

Table 1. Cancer Associated Characteristics[a]

					receptor status (%)		
sample no.	age	istological type	istological grade	Her2/neu	Er	PGR	Ki-67
1	59	IDC	3	1+ neg	90	10	35
2	46	IDC	3	1+ neg	60	40	50
5	37	IDC	3	1+ neg	20	0	40
7	67	ILC + LCIS	2	2+ neg (FISH n.a.)	90	10	25
8	52	IDC	3	2+ neg (FISH n.a.)	0	0	80
9	64	IDC + DCIS	3	1+ neg	60	70	20
10	86	ILC	2	1+ neg	0	0	65
11	58	LCIS	2	2+ neg (FISH n.a.)	95	80	30
12	83	ILC	2	1+ neg	95	80	8
13	38	IDC + DCIS	2	2+ neg (FISH n.a.)	90	60	8
14	84	IDC	2	1+ neg	95	95	12
15	67	IDC	2	0 neg	100	100	10
16	54	IDC	3	1+ neg	90	60	35
17	38	IDC	3	0 neg	0	0	50
18	52	IDC	3	1+ neg	50	5	25
19	76	IDC	3	1+ neg	80	50	40
20	59	IDC	3	1+ neg	90	70	25
22	55	IDC	2	0 neg	95	90	6
23	75	DCIS	2	0 neg	90	80	25
24	34	IDC	3	1+ neg	1	1	40
25	67	IDC	3	3+ pos	95	15	35
27	77	IDC + ILC	2	0 neg	80	70	20
28	69	ILC + LCIS	2	0 neg	80	80	20
29	52	IDC	3	3+ pos	95	95	35
30	50	IDC + DCIS	2	0 neg	*90*	*90*	*5*
32	50	IDC	3	3+ pos	0	0	30
38	67	IDC	3	0 neg	2	2	35
39	57	IDC	3	3+ pos	10	0	40

[a] IDC, infiltrating ductal carcinoma; DCIS, in-situ ductal carcinoma; ILC, infiltrating lobular carcinoma; LCIS, in-situ lobular carcinoma; ER, Estrogen Receptor; PGR, Progesteron Receptor; Ki67, Proliferative index; Her2/neu, amplification status of c-ERB gene; FISH, Fluorescence in situ hybridization.

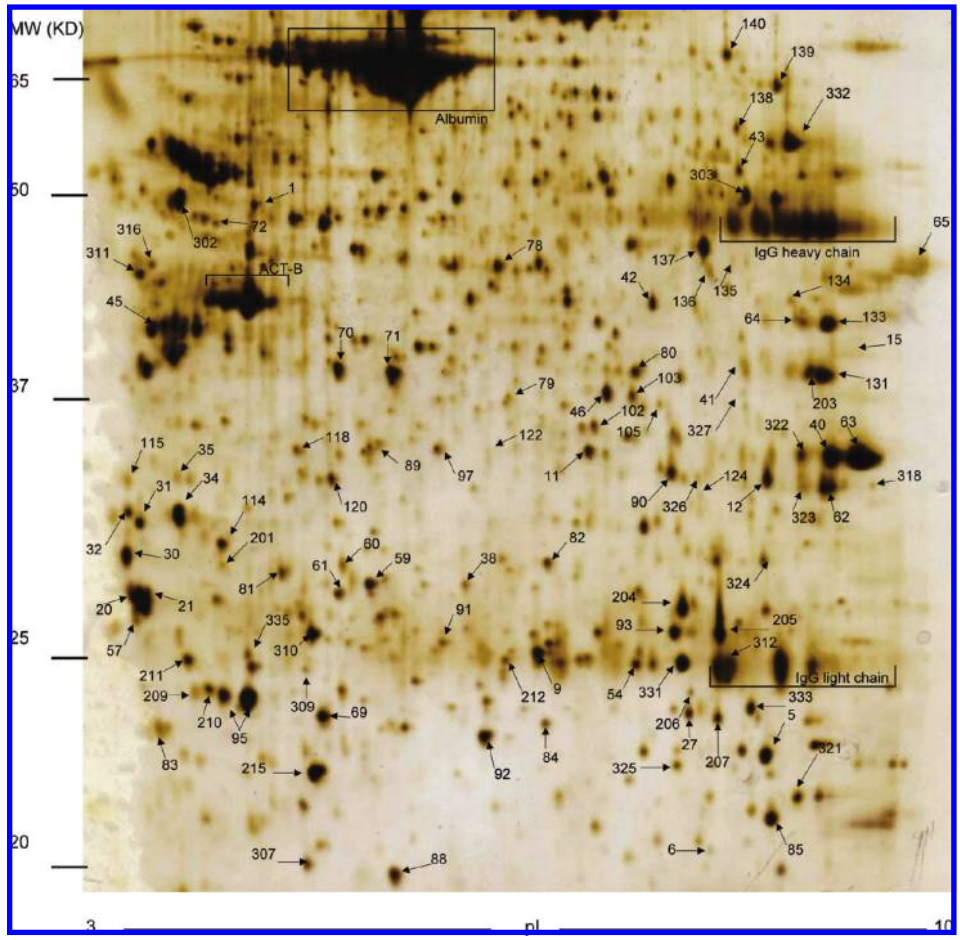

Figure 1. Differentially expressed proteins in TIF of breast cancer biopsies, obtained before chemotherapy. The 2D-electrophoresis gel is representative of all the TIF samples, since it has been obtained by pooling TIF of all patients. Spot number reflects the number listed for the specific protein in Table 2. Molecular weight (kDa) and isoelectric values (p*I*) are shown on the image.

to all the nuclei of the neoplastic cells, independently from the staining intensity.

Statistics. To avoid including in the data analysis proteins with no real changing in the expression, we selected only spots with a fold-change higher than 1.5 to be considered for statistical analysis. A supervised cluster analysis was performed. Following this procedure, the proteins were clustered depending on their expression and on the degree of cluster association considering the type of tissue (TIF or NIF), or on the degree of cluster association considering the response to therapy (responders and nonresponders). Clustering and relevance of selected proteins were disciplined by "PEnalized LOgistic Regression Analysis" (PELORA).

Results

Characterization of Protein in TIF and NIF. Data concerning age of the patients, histological type, histological grade, HER-2/neu amplification status, estrogen and progesterone receptors status, and proliferative index (Ki-67) are given in Table 1. TIF and NIF collected from mammary tissue samples were analyzed by 2-DE as described Experimental Procedures. Figure 1 shows the 2-DE gel obtained by mixing together TIF of all patients, to give a representative picture of proteins spots obtained (for statistical analysis, each sample was analyzed by 2-DE and every single gel is shown in Supplementary Figure 1S in Supporting Information). A large number of protein spots was separated on each 2-DE gel, and out of these visualized protein spots, 140 spots were excised and subjected to ESI-Q-TOF-MS/MS analysis. Keratin spots were present in a moderate amount in all samples. A total of 122 proteins were identified in both TIF and NIF proteome map as representing 55 unique proteins. These are described in Table 2, where panel 1 denotes the 2-DE gel image spot number as illustrated in Figure 1, associated with a commonly used protein name (panel 2) and entry name (panel 3) and SWISS-PROT primary protein accession numbers (panel 4), as identified by MS analysis. Panel 5 lists the appropriate function for each protein as a result of an extensive literature search, utilizing literature references of Swiss-Prot/TrEMBL (http://www.expasy.org) and the SWISS-PROT annotation. Panel 6 indicates the protein localization in the cell; panel 7 represents the theoretical MW of the unprocessed protein, in terms of primary sequence, and panel 8 the p*I* of the protein. Panel 9 reports the highest scores, where score is $[-10 \log(P)]$ and P is the absolute probability that the observed match between the experimental data and the database sequence is a random event, obtained with MASCOT for all proteins listed. Finally, panel 10 refers to the number of peptides matched, and panel 11 shows the sequence coverage, that is, the percentage of amino acids sequenced for the identified protein. Supplementary Table 1S in Supporting Information shows the amino acid sequence of all the identified proteins.

Table 2. Identification of Protein Spots by Mass Spectrometry

spot no.	protein full name	entry name	acc. no.	localization	MW (kDa)	p*I*	score	peptide match	seq. cov.%
135	EH domain-containing protein 2	EHD2	Q9NZN4	membrane	61.3	6.03	191	15	24
321	Heterogeneous nuclear ribonucleoprotein A1	ROA1	P09651	cytoplasm, nucleus	38.9	9.26	90	10	22
35	Heterogeneous nuclear ribonucleoprotein K	HNRPK	P61978	cytoplasm nucleus	51.2	5.39	37	3	7
333	Heterogeneous nuclear ribonucleoproteins A2/B1	ROA2	P22626	nucleus	37.5	8.97	80	6	18
92	Protein DJ-1	PARK7	Q99497	cytoplasm, nucleus	20.1	6.33	43	13	55
201	AMBP protein	AMBP	P02760	secreted	39.9	5.95	45	2	7
309	Immunoglobulin kappa light chain VLJ region	KV302	P01621 (BAC01696)	secreted	11.9	8.7	36	3	39
312	Immunoglobulin kappa light chain VLJ region	KV309	P01621 (BAC01695)	secreted	12.7	4.85	51	2	7
30	14−3−3 protein epsilon	1433E	P62258	cytoplasm	29.3	4.63	94	4	11
20	14−3−3 protein Z/delta	1433Z	P63104	cytoplasm	27.9	4.73	32	4	18
45	40 S ribosomal protein SA	RSSA	P08865	cytoplasm	32.9	4.79	204	6	21
43	Adenylyl cyclase-associated protein 1	CAP1	Q01518	membrane	52.2	8.27	98	6	14
11	Annexin A1	ANXA1	P04083	cytoplasm	38.9	6.57	171	9	27
318−12−326	Annexin A2	ANXA2	P07355	secreted	38.8	7.57	534	23	43
34	Annexin A5	ANXA5	P08758	cytoplasm	36.0	4.94	102	7	16
95	Apolipoprotein A-I	APOA1	P02647	secreted	30.8	5.56	179	12	46
120	Apolipoprotein E	APOE	P02649	secreted	36.2	5.65	134	10	22
140−18−66−217	Complement C3	CO3	P01024	secreted	188.6	6.02	592	31	15
207	GTP- binding nuclear protein RAN	RAN	P62826	nucleus cytoplasm	24.6	7.01	120	13	38
60	N(G),N(G)-dimethylarginine dimethylaminohydrolase 2	DDAH2	O95865	cytoplasm, membrane	29.9	5.66	39	6	27
85−8	Phosphatidylethanolamine-binding protein 1	PEBP1	P30086	cytoplasm	21.2	7.01	172	13	47
86	Programmed cell death protein 6	PDCD6	O75340	membranes	21.9	5.16	106	5	20
210	Rho-GDP dissociation inhibitor 2	GDIR2	P52566	cytoplasm	23.0	5.1	105	11	21
136	6-phosphogluconate dehydrogenase, decarboxylating	6PGD	P52209	cytoplasm	53.6	6.8	214	13	22
84	Acyl-protein thioesterase 1	LYPA1	O75608	cytoplasm	25.0	6.29	172	6	20
102	Aflatoxin B1 aldehyde reductase member 2	ARK72	O43488	cytoplasm	40.0	6.7	178	8	21
46−108	Alcohol dehydrogenase [NADP+]	AK1A1	P14550	cytoplasm	36.9	6.32	61	4	12
15	Alcohol dehydrogenase 1B	ADH1B	P00325	cytoplasm	40.7	8.63	74	8	22
41	Alcohol dehydrogenase class 3 c chain	ADHX	P11766	cytoplasm	40.6	7.45	38	3	5
327	Aldo-keto reductase family 1, member C1	AK1C1	Q5SR14		37.2	8.02	45	4	9
79	Biliverdin reductase A	BIEA	P53004	cytoplasm	33.7	6.06	115	10	32
5−52	Biliverdin reductase B	BLVRB	P30043	cytoplasm	22.2	7.13	128	4	28
204	Carbonic anhydrase 1	CAH1	P00915	cytoplasm	28.9	6.59	327	26	60
205	Carbonic anhydrase 2	CAH2	P00918	cytoplasm	29.3	6.87	372	27	50
138	Catalase	CATA	P04040	peroxisome	59.9	6.9	288	22	32
209	Catechol O-methyltransferase	COMT	P21964	cytoplasm, membrane	30.5	5.26	182	6	25
203−131	Fructose- bisphosphate aldolase A	ALDOA	P04075	cytoplasm, nucleus, exosome	39.9	8.3	377	28	64
103	Fructose-1,6-bisphosphatase 1	F16P1	P09467	cytoplasm	37.2	6.54	88	5	24
335	Glutathione S-transferase Mu 3	GSTM3	P21266	cytoplasm	27.0	5.37	66	5	18
38	Glutathione transferase omega-1	GSTO1	P78417	cytoplasm	27.8	6.23	65	4	13
63−40−322	Glyceraldehyde-3-phosphate dehydrogenase (GAPDH)	G3P	P04406	cytoplasm	36.2	8.57	245	8	31
73−122	Glycerol-3-phosphate dehydrogenase [NAD+], cytoplasmic	GPDA	P21695	cytoplasm	38.2	5.81	86	8	24
3	Hemoglobin subunit beta	HBB	P68871	cytoplasm	16.1	6.75	32	4	29
42	Isocitrate dehydrogenase [NADP] cytoplasmic	IDHC	O75874	cytoplasm	46.9	6.53	113	7	14
62 - 323	L-lactate dehydrogenase A chain	LDHA	P00338	cytoplasm	37.0	8.44	170	10	30
89	L-lactate dehydrogenase B chain	LDHB	P07195	cytoplasm	36.9	5.71	156	9	24
90−14	Malate dehydrogenase, cytoplasmic	MDHC	P40925	cytoplasm	36.6	6.91	40	3	10
124	Monoglyceride lipase	MGLL	Q99685	cytoplasm	33.5	6.49	94	3	14
325	Peroxiredoxin - 1	PRDX1	Q06830	cytoplasm	22.3	8.27	110	10	43
215	Peroxiredoxin - 2	PRDX2	P32119	cytoplasm	22.0	5.66	211	16	42

Table 2. Continued

spot no.	protein full name	entry name	acc. no.	localization	MW (kDa)	p*I*	score	peptide match	seq. cov.%
9−56	Peroxiredoxin - 6	PRDX6	P30041	cytoplasm	25.1	6	77	9	40
64−133	Phosphoglycerate Kinase 1	PGK1	P00558	cytoplasm	45.0	8.3	136	10	24
93	Phosphoglycerate mutase 1	PGAM1	P18669	cytoplasm	28.9	6.67	137	13	52
332	Pyruvate kinase isoenzymes M1/M2	KPYM	P14618	cytoplasm	58.5	7.96	141	12	28
79−104	Transaldolase	TALDO	P37837	cytoplasm	37.7	6.36	119	5	16
54−94−212−214−331	Triosephosphate isomerase	TPIS	P60174	cytoplasm	26.9	6.45	783	50	65
21	14−3−3 protein gamma	1433G	P61981	cytoplasm	28.5	4.8	59	4	13
2	Actin, cytoplasmic 1	ACTB	P60709	cytoplasm	42.1	5.29	109	8	21
24	Actin-related protein 2/3 complex subunit 4	ARPC4	P59998	cytoplasm	19.8	8.53	79	4	22
137	Alpha-enolase	ENOA	P06733	cytoplasm, membrane, nucleus	47.5	7.01	176	12	32
48−10	Cofilin-1	COF1	P23528	cytoplasm	18.7	8.22	142	10	35
47	Destrin	DEST	P60981	cytoplasm	19.0	8.06	68	2	13
77	Dynactin subunit 2	DCTN2	Q13561	cytoplasm, membrane	44.3	5.1	72	5	14
118	F-actin-capping protein subunit alpha-1	CAZA1	P52970	cytoplasm	33.1	6.45	52	5	24
69	Glutathione S-transferase P	GSTP1	P09211	cytoplasm	23.6	5.43	86	6	42
324	Guanine nucleotide-binding protein subunit b-2-like 1	GBLP	P63244	cytoplasm, membrane	35.5	7.6	135	6	16
88	Nucleoside diphosphate kinase A	NDKA	P15531	cytoplasm, nucleus	17.3	5.83	84	7	18
23	Nucleoside diphosphate kinase B	NDKB	P22392	cytoplasm, nucleus	17.4	8.52	75	6	26
61	Platelet-activating factor acetylhydrolase IB subunit beta	PA1B2	P68402	cytoplasm	25.7	5.57	82	2	12
27	Proteasome subunit alpha type-2	PSA2	P25787	cytoplasm nucleus	26.0	6.92	35	2	7
211	Rho- GDP dissociation inhibitor 1	GDIR1	P52565	cytoplasm	23.3	5.02	122	9	23
83	Translationally controlled tumor protein	TCTP	P13693	cytoplasm	19.7	4.48	123	5	15
31	Tropomyosin a −3 chain	TPM3	P06753	cytoplasm, cytoskeleton	32.9	4.68	132	6	16
32	Tropomyosin a-4 chain	TPM4	P67936	cytoplasm, cytoskeleton	28.6	4.67	90	3	13
302	Tubulin, b polypeptide	TBB5	P07437	cytoplasm	50.1	4.78	96	6	12
311−316	Vimentins	VIME	P08670	cytoplasm	53.7	5.06	76	10	1 6
105	26S proteasome non-ATPase regulatory subunit 7	PSD7	P51665	cytoplasm nucleus	37.1	6.29	37	3	10
97	60 S acid ribosomal protein P0	RLA0	P05388	cytoplasm	34.4	5.71	211	20	51
6	a crystalline b chain (HspB5)	CRYAB	P02511	cytoplasm	20.1	6.76	51	5	21
134	Argininosuccinate synthase	ASSY	P00966	cytoplasm	46.8	8.08	181	15	39
65	Elongation factor 1-a 1	EF1A1	P68104	cytoplasm	50.5	9.1	142	8	12
70−71−303	Fibrinogen b chain	FIBB	P02675	secreted	56.6	8.54	390	19	30
91	Heat shock protein b 1	HSPB1	P04792	cytoplasm nucleus	22.8	5.98	260	19	40
115	Polymerase I and transcript release factor	PTRF	Q6NZI2	cytoplasm, membrane	43.5	5.51	56	1	4
59	Proteasome Activator complex subunit 1	PSME1	Q06323	cytoplasm, nucleus	28.9	5.78	170	10	32
81	Proteasome activator complex subunit 2	PSME2	Q9UL46	cytoplasm	27.4	5.44	57	4	17
82	Proteasome subunit a type 1	PSA1	P25786	cytoplasm nucleus	29.8	6.15	79	12	29
57	Proteasome subunit alpha type-5	PSA5	P28066	cytoplasm nucleus	26.6	4.74	44	2	7
206	Protein-L-isoaspartate(D-aspartate) O-methyltransferase	PIMT	P22061	cytoplasm	24.8	6.7	42	3	18
310	Serum amyloid P-component	SAMP	P02743	secreted	25.5	6.1	47	5	21
80	Sialic acid synthase	SIAS	Q9NR45	cytoplasm	40.7	6.29	130	5	15
78	T-complex protein 1 subunit beta	TCPB	P78371	cytoplasm	57.8	6.01	51	7	10
139−44	Transketolase	TKT	P29401	cytoplasm	68.5	7.58	372	32	38
114−58	Chloride intracellular channel protein 1	CLIC1	O00299	cytoplasm, nucleus, membrane	27.2	5.09	181	7	31
307	Ferritin light chain	FRIL	P02792	cytoplasm	20.1	5.51	244	21	40
87−17−55−200−202	Serum albumin	ALBU	P02768	secreted	71.3	5.92	294	35	49
1	Vitamin D-binding protein	VTDB	P02774	secreted	54.5	5.4	46	5	11

Table 3. Changes in Protein Expression in TIF Compared to NIF

protein name	fold change
Nucleic Acid Metabolism	
PARK 7	1.32
Signal Transduction; Cell Communication	
14−3−3-E	1.52
14−3−3-Z	1.58
APO A1 sx	−2.40
ANXA 5	1.52
APO A1 dx	−1.33
PEBP 1	−1.33
ANXA 2	−2.89
Energy Pathways	
PRDX 2	−2.97
APO E	−1.51
TPIS (spot no. 212)	1.40
PRDX 6	−1.77
TPIS (spot no. 331)	2.05
PGAM 1	−2.81
CAH 1	−2.51
CAH 2	−1.73
BLVRB	−2.02
LDHA sx	−1.75
G3P sx	2.01
ALDO A sx	1.28
PGK 1 sx	−2.83
LDHA dx	−1.79
G3P cn	1.85
G3P dx	1.08
PGK 1 dx	3.47
ALDO A dx	2.06
ADH 1B	−4.66
Cell Growth and/or Maintenance	
14−3−3-G	3.37
TPM 4	1.21
TPM 3	1.01
VIME (spot no. 311)	1.05
VIME (spot no. 316)	1.18
TBB 5	2.11
GSTP 1	1.52
Protein Metabolism	
PSA 5	3.10
LDHB	−1.80
FIBB sx	−4.08
FIBB dx	−3.05
HSPB 1	−3.61
CRYAB	−17.74
EF 1a	−1.09

Table 3 indicates proteins with a different expression in TIF with respect to NIF, as resulted from PD-Quest analysis. In the group of proteins involved in nucleic acid metabolism, we found only a slight increase in TIF of PARK 7 expression. Proteins belonging to the energy pathways group show different expression profile: ADH-1B, CAH 1, PRDX 2, LDHA, LDHB, APO E, PRDX 6, PGAM 1, CAH 2, BLVRB and PGK 1 sx have a variable degree of reduced expression in TIF; ALDO-A, G3P, PGK1 dx, TPIS and show an increased expression. In the cell growth and/or maintenance group, we found that 14−3−3-G was increased 3.37-fold, tubulin β polypeptide (TBB 5) 2.11-fold, tropomyiosin 3 and 4 (TPM 3 and 4) 1.01- and 1.21-fold, vimentines (VIME) 1.05- and 1.18-fold, and glutathione-S transferase-P (GSTP1) 1.52-fold. In protein metabolism group, we found an increased expression (3.10-fold) of PSA 5, while

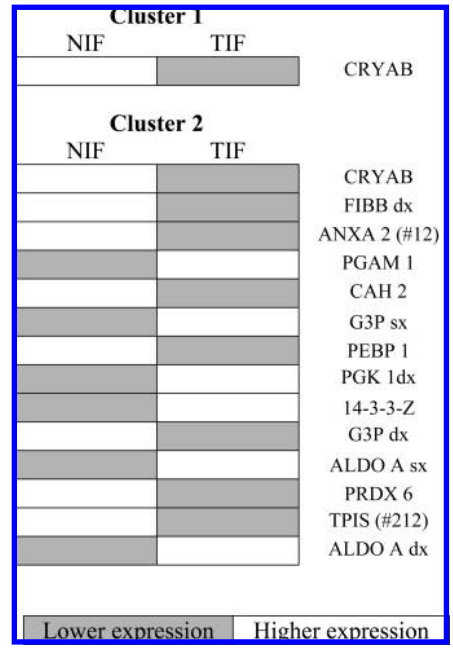

Figure 2. Proteins expression level in supervised cluster analysis. Fourteen proteins were clustered in two groups (cluster 1 and cluster 2, each including, respectively, 1 and 14 proteins). Different colors indicate different expression level.

all the other proteins show a reduced expression, especially CRYAB, which expression is reduced 17.74-fold. Among the signal transduction proteins, we found a general decrease of the APO A1, PEBP 1 and ANXA 2, while ANXA 5 and the enzymatic proteins, 14−3−3 E and 14−3−3 Z, were enhanced. The subsequent hierarchical cluster analysis indicated the presence of two clusters of significantly differentially expressed proteins. Figure 2 shows the supervised cluster analysis, conducted comparing protein differentially expressed in TIF with respect to NIF (different colors represent differentially expressed proteins). This allowed the identification of two clusters containing, respectively, one and 14 proteins. Cluster 1 contains CRYAB protein (final criterion 11.900), which shows a reduced expression in TIF respect to NIF. Cluster 2 (final criterion 6.842) contains CRYAB and also ANXA2, FIBBdx, CAH 2, PEBP 1, G3Pdx, PRDX 6 and TPIS, all showing a reduced expression. Proteins with an increased expression were PGAM 1, G3Pcn, PGK1, 14−3−3-Z, and ALDO A.

Proteins Expressed in NIF and TIF before CHT: Comparison between Responders and Nonresponder Patients. Fourteen patients out of the 28 considered for the 2-DE analysis of TIF and NIF underwent chemotherapy. Not all the patients had a satisfactory response to the chemotherapy, evaluated as tumor size reduction: 10 had more than 50% of reduction in size, measured at the ultrasound and mammographic examinations, indicating a good response to therapy, and four had no reduction of tumor size. Proteins isolated in TIF and NIF of both group of these patients (10 responders and 4 nonresponders, as illustrated in Supplementary Figure 1S) before chemotherapy were pooled and processed by 2-DE to have a representative picture of the expression patterns (Figure 3). Analysis of spots intensity by PD-QUEST software shows changes in protein expression in TIF respect to NIF, in both groups of patients (responders and nonresponders). Referring to Table 4, column A, we can appreciate that the antiapoptotic protein CRYAB is down-

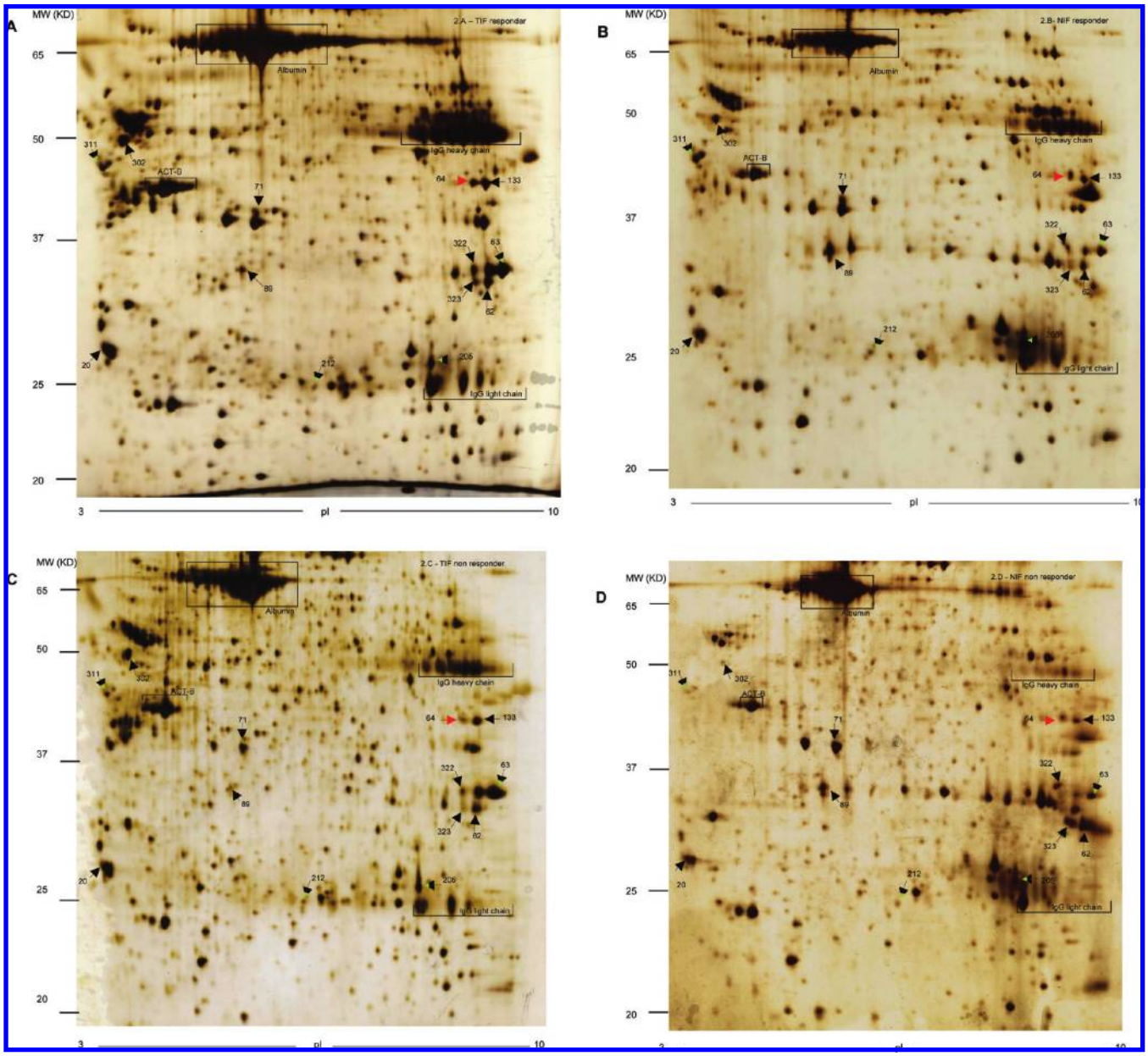

Figure 3. 2-DE imagines of protein pools in TIF and NIF of breast cancer biopsies, obtained before chemotherapy. Molecular weight (kDa) and isoelectric values (p*I*) are shown on the image. Arrows indicate proteins identified by cluster analysis (as illustrated in Figure 4B) of patients before CHT (different arrows indicate different clusters: green arrow, cluster 1; red arrow, cluster 2; black arrow, cluster 1 and 2). (A) TIF of responders; (B) NIF of responders; (C) TIF of nonresponders; (D) NIF of nonresponders.

regulated in TIF with respect to NIF in both responders and nonresponders, even though the degree of down-regulation is higher in this latter group. Almost same behavior is seen for FIBB sx, HSPB 1, ANXA 2 and ADH 1B, while several others are down-regulated in TIF with respect to NIF at almost the same extent in both groups of patients. A certain number of proteins are overexpressed in TIF of both groups: 14−3−3-E, 14−3−3-Z, TPIS, G3P sx and cn, PGK 1 dx, ALDO A dx, 14−3−3-G, TBB 5, and GSTP 1. Among these, PGK 1dx and ALDO A dx show a more relevant level of overexpression in TIF respect to NIF in patients nonresponders to CHT. Proteins down-regulated in TIF of responders and overexpressed in TIF of nonresponders are: PARK 7, ANXA 5, G3P dx, TPM 3, EF 1A. In contrast, proteins overexpressed in TIF of responders and down-regulated in TIF of nonresponders are APO A1 dx and sx, PEP 1, PRDX 6, PGAM 6, ALDO A sx, TPM 4, VIME, and PSA 5.

Considering again Table 4, in column B, two other types of comparison are made to evaluate differences in protein expression profile in the two groups of patients both in NIF and in TIF.

Responder patients, in contrast to nonresponders, show an increased expression in NIF of protein PARK7, which is involved in cell growth, while in TIF, it is slightly down-regulated. Most of the protein belonging to the signal transduction are down-regulated in NIF of responders. In particular, comparing responders versus nonresponders, we found that proteins 14−3−3-Z and ANXA 5 are down-regulated in both NIF and

Table 4. Changes in Protein Expression

	A		B	
	TIF vs NIF		responders vs nonresponders	
	responders	nonresponders	NIF	TIF
	Nucleic Acid Metabolism			
PARK 7	−1.07	2.03	1.87	−1.16
	Signal Transduction; Cell Communication			
14−3−3-E	1.22	1.83	1.05	−1.43
14−3−3-Z	1.22	1.73	−2.49	−3.54
APO A1 sx	1.58	−5.49	−4.95	1.76
ANXA V	−1.01	1.99	−1.10	−2.21
APO A1 dx	1.65	−2.61	−2.45	1.76
PEBP 1	1.21	−2.30	−1.44	1.93
ANXA 2	−1.61	−5.10	−1.82	1.74
	Energy Pathways			
PRDX 2	−3.24	−2.54	1.98	1.55
APO E	−1.38	−1.94	2.49	3.50
TPIS (no. 212)	1.14	2.34	3.67	1.79
PRDX 6	1.21	−3.04	−2.70	1.36
TPIS (no. 331)	1.29	3.17	1.49	−1.65
PGAM 1	1.84	−6.70	−7.14	1.72
CAH 1	−2.38	−2.64	−1.20	−1.08
CAH 2	−2.50	−1.22	1.35	−1.53
BLVRB	−2.29	−1.46	3.25	2.08
LDHA sx	−1.96	−1.65	−1.56	−1.85
G3P sx	2.24	1.67	1.50	2.00
ALDO A sx	3.89	−3.23	−2.67	4.70
PGK 1 sx	−1.70	−3.86	−2.46	−1.09
LDHA dx	−1.54	−1.95	−1.96	−1.54
G3P cn	3.12	1.30	−2.27	1.06
G3P dx	−1.01	1.15	−1.08	−1.25
PGK 1 dx	2.60	5.53	2.39	1.13
ALDO A dx	1.04	4.18	2.08	−1.93
ADH 1B	−2.81	−8.39	−1.49	2.01
	Cell Growth and/or Maintenance			
14−3−3-G	3.27	3.54	1.68	1.55
TPM 4	1.45	−1.01	−1.16	1.26
TPM 3	−1.13	1.09	−1.55	−1.91
VIME (no. 311)	2.57	−1.41	−4.47	−1.23
VIME (no. 316)	1.97	−1.24	−2.11	1.15
TBB 5	2.11	2.13	3.98	3.94
GSTP 1	1.96	1.25	−1.65	−1.06
	Protein Metabolism			
PSA 5	9.39	−2.03	−2.42	7.88
LDHB	−1.43	−2.45	1.01	1.73
FIBB sx	−1.68	−7.57	−3.10	1.45
FIBB dx	−3.17	−2.87	1.72	1.55
HSPB 1	−2.05	−7.61	−1.46	2.55
CRYAB	−13.20	−25.94	−1.09	1.81
EF 1a	−1.87	2.04	2.92	−1.31

TIF of responders; APO A1 sx, APO A1 dx, PEBP 1 and ANXA 2 are down-regulated in NIF and up-regulated in TIF of responders, and protein 14−3−3-E is up-regulated in NIF and down-regulated in TIF of responders.

Considering proteins belonging to the energy pathways, we found that responders, in contrast to nonresponders, present in both NIF and TIF an increased expression of PRDX 2, APO E, TPIS, BLVRB, G3P sx, PGK 1 dx, and a decreased expression of CAH 1, LDHA sx, LDHA dx, PGK 1 sx, and G3P dx. Of relevance is the presence in NIF of responders in contrast to nonresponders of a decreased expression of PGAM 1 and an increased expression of ALDO A sx in TIF.

In the group of proteins involved in cell growth and/or maintenance, it is of relevance the increased expression in both NIF and TIF of responders of TBB5, and the decrease (more relevant in NIF) of VIME.

In the protein metabolism class, the Elongation Factor 1-alpha, which is involved in protein biosynthesis, presents a higher expression in NIF of responders; meanwhile, a lower expression is observed in TIF. Responders show also a decreased expression in NIF of PSA 5 (which is, on the contrary, highly increased in TIF) and FIBB sx.

A statistical analysis has been conducted comparing protein expressed in interstitial fluids of responder and nonresponder patients, without discrimination between tumor or normal tissue. Forty-two protein spots, differentially expressed in responders and nonresponders, were adopted for hierarchical cluster analysis: clustergram is shown in Figure 4, panel A,

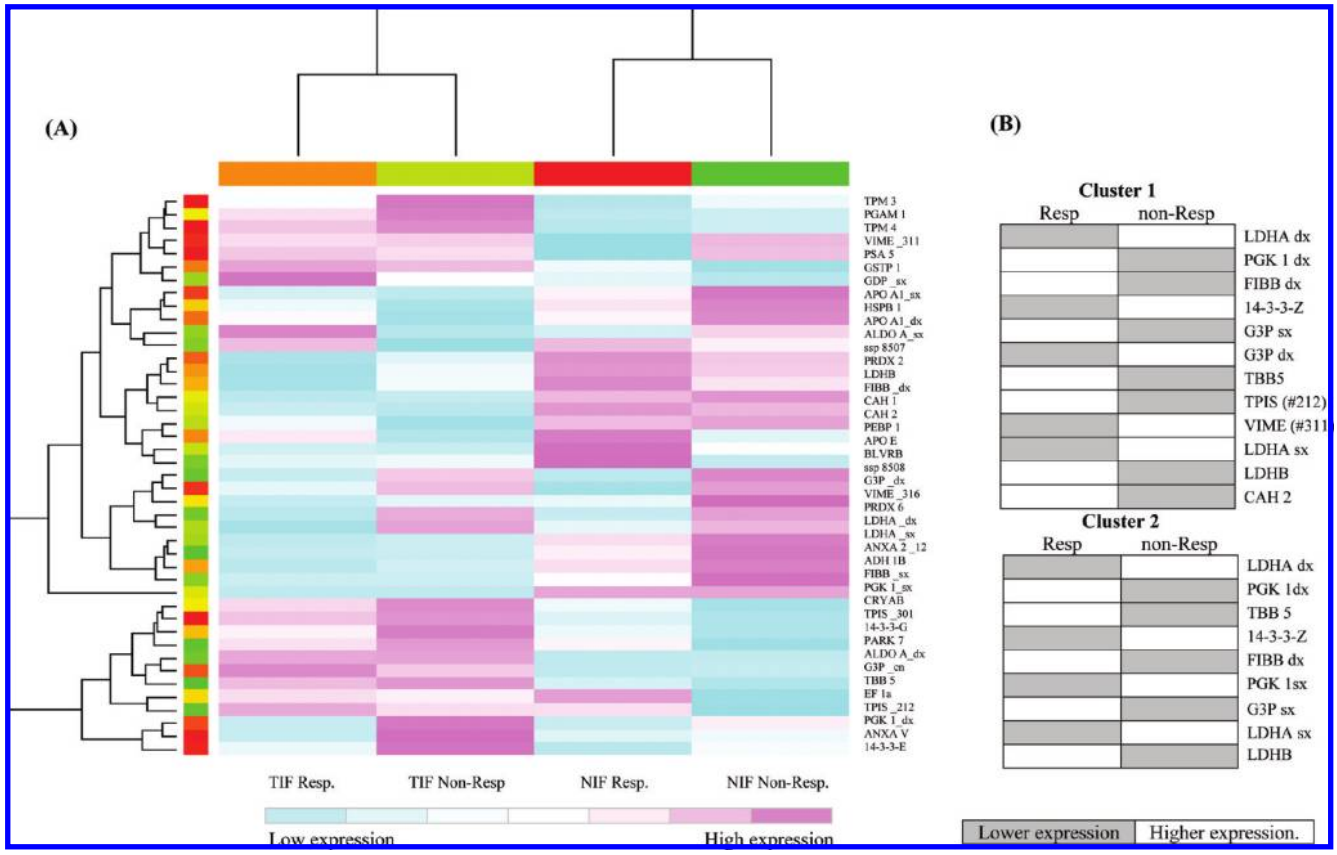

Figure 4. Visualization of putative biomarkers of chemotherapy response. (A) Hierarchical cluster analysis, where complete linkage for treatment response is analyzed. This clustergram was constructed from 42 differentially expressed spots in patients responders vs nonresponders and TIF and NIF have been considered individually. In scale bar, different colors indicate different expression of the selected proteins: turquoise indicates low expression and fuchsia high expression. (B) Proteins level in supervised cluster analysis. Thirteen proteins were clustered in two groups (cluster 1 and cluster 2, each including, respectively, 12 and 9 proteins). Different colors indicate different protein expression: lower (gray) and higher (white) expression.

where different colors represent differentially expressed proteins. Subsequently, a supervised cluster analysis (panel B) was applied for identification of protein clusters predictive of CHT response. Two significant clusters have been identified: cluster 1 contains 12 proteins (LDH A dx and sx, PGK 1 dx, FIBB dx, G3P dx and sx, TBB5, TPIS, LDHB, CAH, VIME, 14−3−3 Z), with a final criterion of 3.083; cluster 2 has nine proteins, which are LDH A dx and sx, LDH B, PGK 1 sx and dx, TBB 5, 14−3−3-Z, FIBB dx, G3P sx, with a final criterion of 2.097. The proteins present in these clusters are indicated by arrows in 2-DE gels of both Figures 3 and 6.

The results of this analysis let us to identify as predictive of CHT response an increase in expression of LDH B, FIBB dx, G3P sx, TBB 5, TPIS, CAH 2, PGK 1dx, coupled with a decreased expression of LDH A, 14−3−3 Z, G3P dx, VIME, and PGK 1sx proteins in interstitial fluid. The magnified 2-DE spots of all these proteins are presented in Figure 5, where the protein spots in every single patient and the localization in the respective interstitial fluid (TIF and NIF) is reported.

Proteins Expressed in NIF and TIF after CHT: Comparison between Responders and Nonresponder Patients. To evaluate whether CHT could modify the expression of proteins identified by supervised cluster analysis, we performed 2-DE analysis of TIF and NIF after CHT. All patients underwent CHT, followed by surgery; at this time, breast tissue samples were obtained and TIF and NIF collected. In Figure 6, the silver stained gels of pooled TIF and NIF are presented. Panel A shows the 2-DE gels of both responders and nonresponders. Comparing these gels with those represented in Figure 3, we can appreciate that proteins' expression in TIF of patients responder to CHT is generally decreased after this treatment; on the contrary, it is enhanced in NIF. Patients nonresponder to CHT show, after chemotherapy, an unchanged expression pattern in TIF and a slightly decreased expression in NIF. Analyzing the single gel spots of the proteins identified by supervised cluster analysis, in panel B of Figure 6, it is possible to evaluate changes in expression induced by CHT. In these histograms, the clustered proteins significantly changed in the expression profile after CHT are presented. In general, expression of clustered proteins was always decreased. Patients responder to CHT show a decreased expression in TIF of most clustered proteins (panel B1), while on the contrary, the nonresponders do not exhibit any modification in TIF (panel B3), with the exception of 14−3−3-Z protein, which is significantly decreased after CHT. In nonresponders, the most important changes are present in NIF (panel B4). In Supplemental Figure 3S, the magnified cluster protein spots of responders and nonresponders pools are presented.

Discussion

The heterogeneity of malignant cells is one of the main hurdles in developing therapies selectively targeting the cancer cell; the characterization of such heterogeneity might be useful

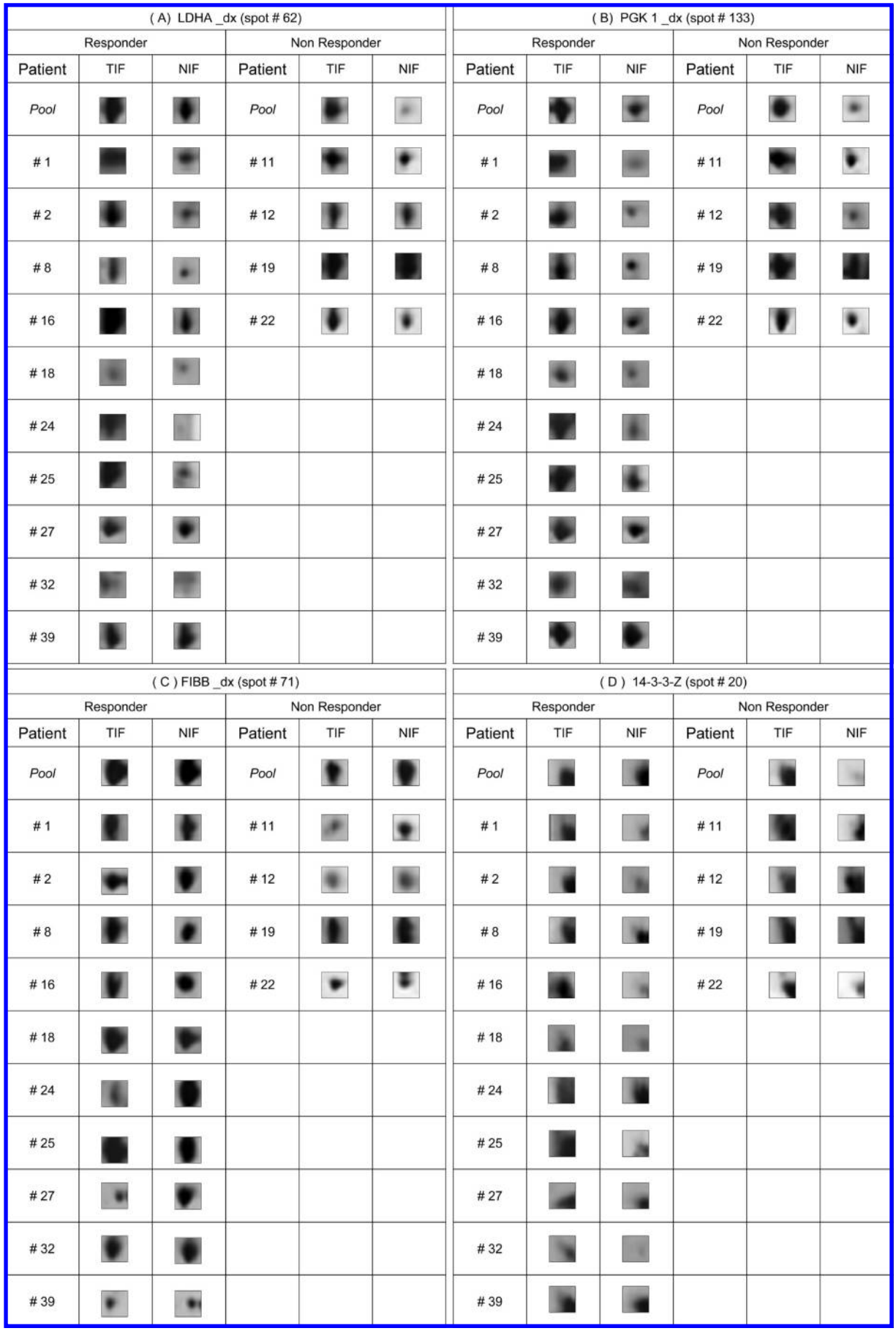

Figure 5. Part 1 of 4. Magnified protein spots in TIF and NIF of responder and nonresponder patients: comparison with the corresponding pool. Each panel corresponds to a different protein, which name is reported on the first line.

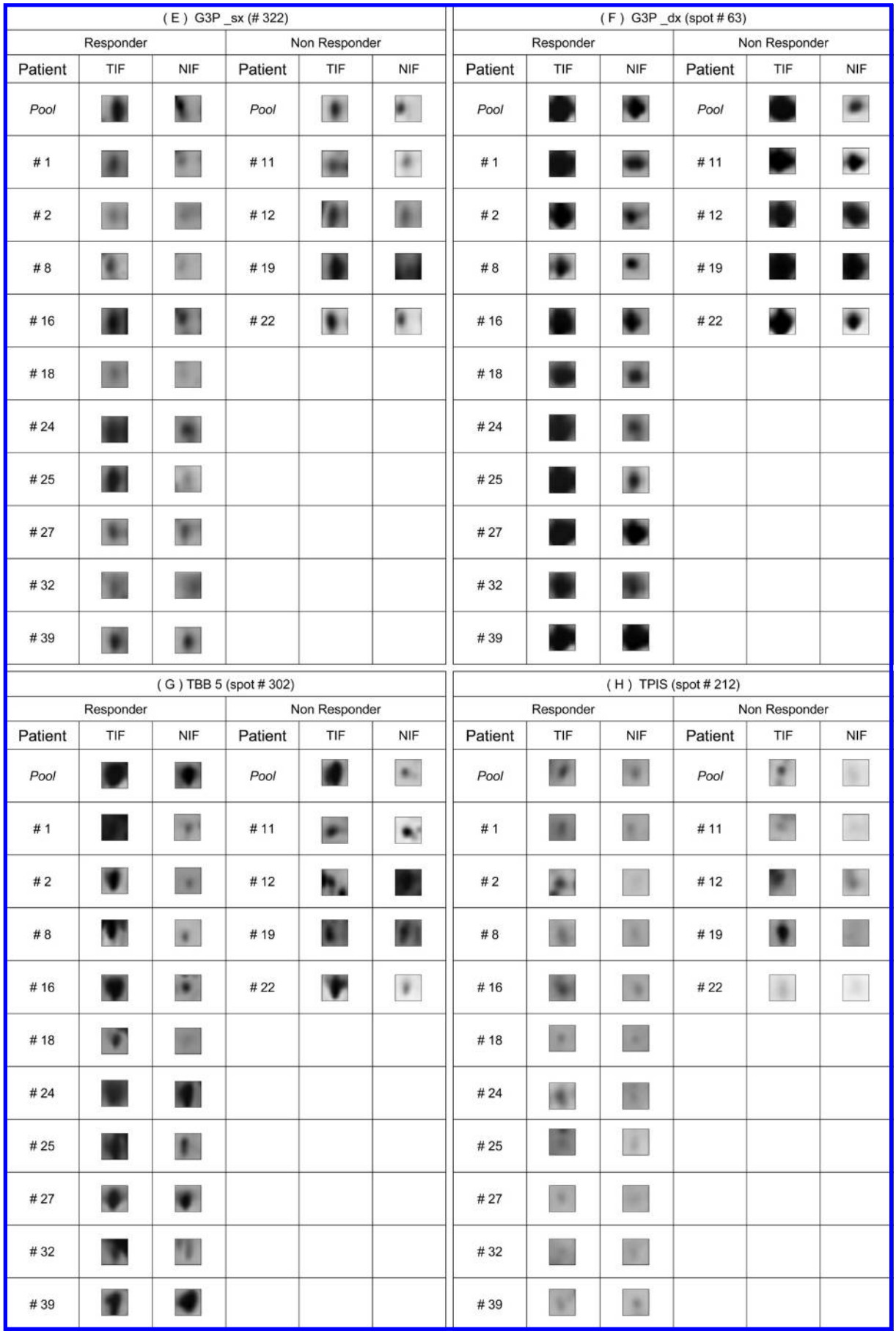

Figure 5. Part 2 of 4.

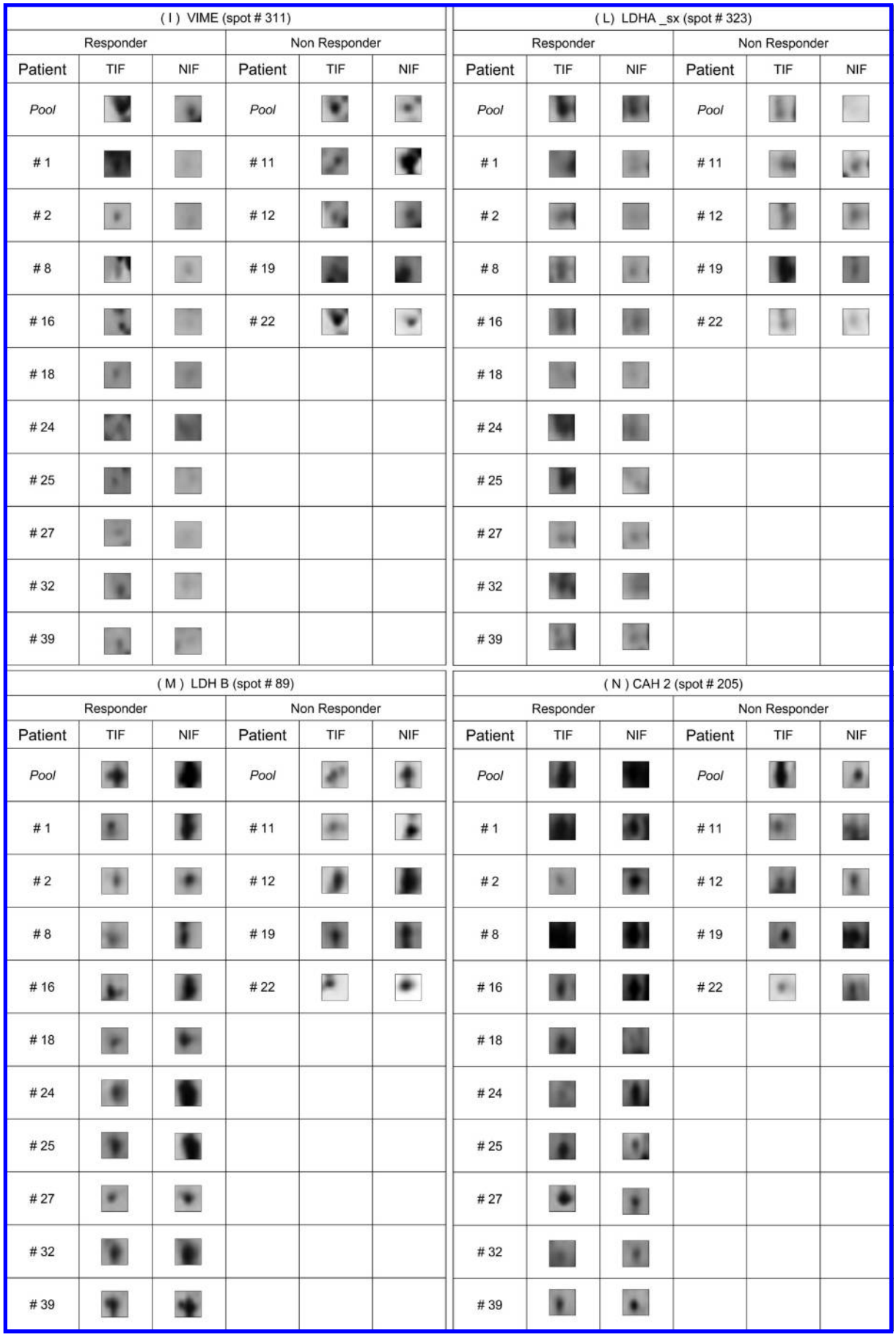

Figure 5. Part 3 of 4.

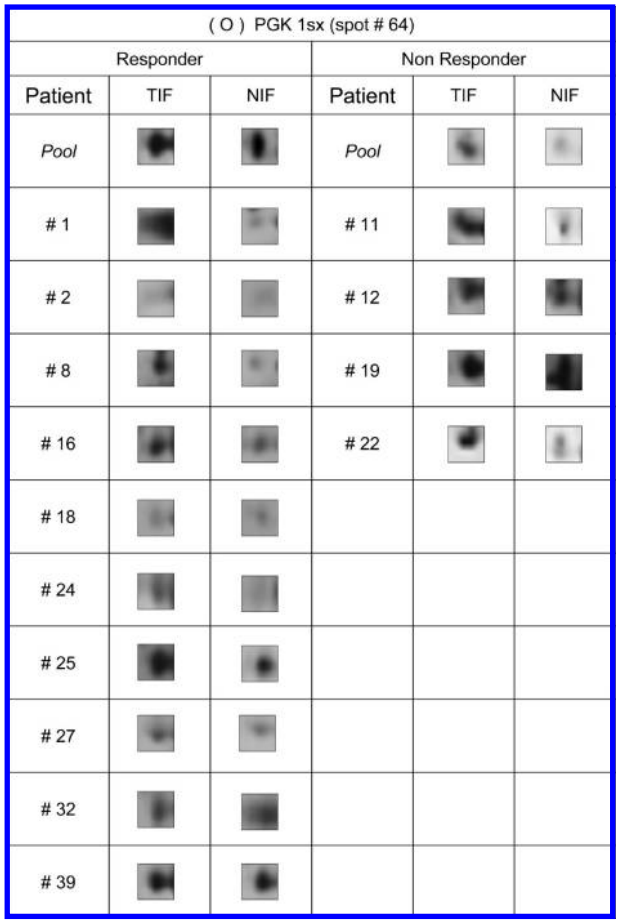

Figure 5. Part 4 of 4.

for selecting the most appropriate therapeutic strategy for each case. With this aim, we evaluated the proteomic profile of 14 breast cancer biopsies using a mass spectrometry based application on proteins separated by 2DE. With this approach, we found a high degree of variation in proteins expression comparing proteins expressed in NIF with proteins expressed in TIF: this can be easily evaluated at a first look of the 2DE gels presented in Figure 3.

Of relevance is the high degree of down-regulation of the antiapoptotic protein CRYAB, which is the unique protein represented in cluster 1. This can be justified by the role of CRYAB in the tyrosine kinase signaling, that could be easily altered in cancer cells: its reduced expression has been already associated with a negative prognosis.[20] On the other hand, also the secreted protein ANXA 2, which is involved in exocitosis process, is reduced. Most of the proteins involved in protein metabolism show a decreased expression in TIF; however, only CRYAB and FIBB are present in clusters. The down-regulation of FIBB could easily indicate the lack of regulation in cell proliferation, which is a well-known characteristic of the tumor cell.

In the energy pathway group, of relevance is the evident decreased expression of PRDX 6 in TIF. This enzyme is involved in hydrogen peroxide detoxification (also the PRDX 2 is decreased in TIF, even though this latter is not present in clusters). Enzymes involved in the glycolytic pathway, such as ALDO A, G3P, PGAM 1, and PGK 1, are overexpressed as expected, since in most human cancer they are concurrently up-regulated. Nevertheless, not all the glycolityc enzymes show a similar expression pattern: as already reported in other studies, some of them are down-expressed and this issue has not yet found an explanation. Among the down-expressed cluster proteins belonging to the glycolytic pathway, there is also CAH 2. Carbonic anhydrases are widespread enzymes, present in mammals in at least 14 different isoforms. In the interstitial fluid, we detected the CAH 1 and CAH 2, which are cytosolic isoforms, while the membrane-bound isoforms (like the CAH 9, CAH 12) were not present. The various isoforms seem to play different roles in prognosis of invasive breast carcinoma: the CAH 9 up-regulation has been associated with resistance to chemotherapy[21] and has been proposed as a predictive marker of poor response to adjuvant treatment.[22,23] On the contrary, CAH 12 up-regulation has been associated with a better prognosis[24] in breast cancer; in contrast with these findings, it has been also demonstrated that its suppression reduces the invasiveness of renal cancer cells.[25] Regarding CAH 2, it has been correlated with aggressiveness of colorectal cancer;[26] it exhibits the same behavior as CAH 12 in renal cancer cell lines[25] and it suppression leads to inhibition of endocrine tumor cells growth.[27] Our study demonstrates that in breast cancer patients the expression of CAH 2 is higher in the normal interstitial fluid that in tumor fluid. The overall expression of this enzyme in cancer patients (without discrimination between TIF and NIF) when increased seems to be predictive of good response to CHT.

Finally, it can be noted that, in both TIF and NIF, albumin is well-represented, indicating the presence of serum in the interstitial fluid, as already reported in the literature.[17,18] We can conclude that the protein profile of TIF is remarkably similar to that of NIF, with interesting differences in the expression of a number of proteins, indicating an alteration in the synthesis of proteins involved in cell proliferation, energy metabolism, transport, and oxidative stress. Clustered proteins could represent a potential resource for diagnostic biomarkers discovery that could be evidenced in serum.

The most relevant part of this work is the search of protein clusters predictive of response to CHT. The potential relevance of this approach is crucial, since it might lead to a personalized and more successful therapy.[28] We proceeded to consider the protein expression profile of TIF and NIF collectively, since microenvironment is also involved in tumor progression. Considering clustered proteins overexpressed in responder patients with respect to the nonresponders, we found that most of these belong to the energy pathways group. This could indicate a potential role of the defense response against tumor. Proteins belonging to the glycolytic pathway (LDH B, PGK 1, G3P, TPIS, CAH2) are present in both clusters, indicating that the induction of this energetic pathway might lead to a positive outcome in cancer treatment. It has been demonstrated that the reason for the increased expression of LDH A observed in gastrointestinal cancer patients is transcriptional silencing of LDH B expression due to aberrant methylation in the promoter region of LDH B.[29] On the contrary, in retinoblastoma cell line, the presence of an aberrant transcription of the LDH A gene, attributable to promoter methylation, has been demonstrated.[30] The progressive increase of LDH B levels in serum of lung cancer patients has been correlated with the clinical stage of the disease.[31] In our study, the increase in responders of LDH B expression might be indicative of a link between a better prognosis and the absence of hypermethylation of the promoter.

Our study indicates that also overexpression of TPIS, which is a homodimeric enzyme catalyzing the interconversion of

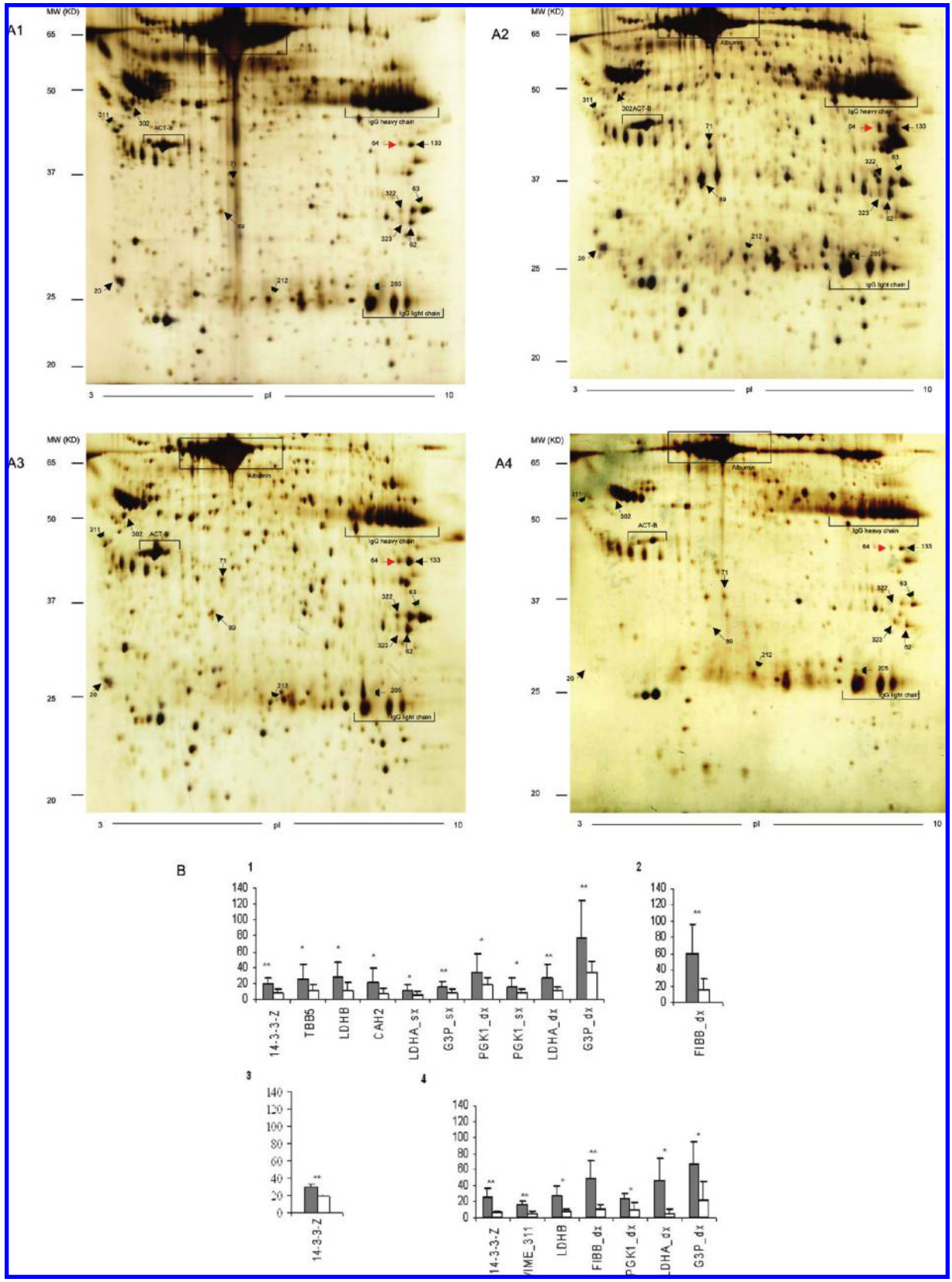

Figure 6. Modification in expression of protein clusters induced by chemotherapy. Panel A shows the 2-DE gel obtained by pooling samples of the same type. Arrows indicate proteins identified by cluster analysis of patients before CHT (different arrows indicate different clusters: green, cluster 1; red, cluster 2; black, cluster 1 and 2). (A1) TIF of responders; (A2) NIF of responders; (A3) TIF of nonresponders; (A4) NIF of nonresponders. Panel B shows the histograms obtained by PD-Quest analysis of clustered proteins, expressed as spot intensity: gray bar, before chemotherapy; white bar,, after chemotherapy. (B1) TIF of responder patients; (B2) NIF of responder patients; (B3) TIF of nonresponder patients; (B4) NIF of nonresponder patients (Student's *t* test: $*p < 0.05$; $**p < 0.01$ of pre- versus postchemotherapy).

D-glyceraldehyde-3-phosphate and dihydroxyacetone phosphate and is involved in glycolysis, gluconeogenesis and triglyceride synthesis,[32] could be predictive of positive response to CHT. Until now, we have a few data on the involvement of this protein in cancer. It has been found overexpressed in HER-2/neu-positive breast cancer,[33] but this finding cannot be used for a comparison with our results, since 89% of our patients where HER.2/neu-negative. There is at least one study where expression of this enzymatic protein has been studied "in vitro" in renal cell carcinoma cell lines: the authors found no differences in the expression profile compared to normal kidney epithelium.[34] We found that another glycolytic enzyme present in both cluster is PGK1 (which is also overexpressed in HER-2/neu-positive breast cancer[33]). We detected two spots of this protein, with a different p*I*, where the dx spot is overexpressed and the sx is down-regulated. The p*I* shift on the left (PGK1sx) could be indicative of a post-translational modification of this protein. Usually, it is the presence of acidic phosphate groups that causes a decrease in the p*I* of phosphorylated proteins and the relative shift to specific p*I* regions, depending on the number and site of phosphorylation. A decrease in the post-translational modification of this glycolytic enzyme could be predictive of a better outcome for breast cancer patients.

A shift in p*I* was found also for G3P, where the modified enzyme was found increased in responders and, on the contrary, the unaltered form was decreased. A further study of post-translational modifications of both PGK1 and G3P is needed to better understand the role in CHT response of these proteins. Another enzyme belonging to the glycolytic pathway and present in cluster 1 is the CAH 2. Considering the protein metabolism group, we found a modification of FIBB expression that could be predictive of CHT response. Many studies, showing FIBB localization to the tumor−host cell interface,[35,36] demonstrated that it is a predominant component in breast tumor stroma, and its deposition is also a common feature of other neoplasia, like mesothelioma,[37] colon cancer,[38] and lymphoma.[39] It has been suggested that the primary source of this extracellular FIBB may be, in part, attributable to endogenous synthesis and deposition. It has been demonstrated that MCF-7 human breast cancer cells synthesize and secrete FIBB, suggesting the origin of FIBB in the stroma of breast carcinoma in vivo.[40] In our study, FIBB is overexpressed in interstitial fluid of responders and most of this protein is expressed in NIF. However, it cannot be excluded that an important source of FIBB is plasma contamination; this critically reduces the relevance of this finding.

Several reports have shown that tubulin expression is correlated "in vitro" with the sensitivity to taxanes.[41−43] Moreover, tubulin beta has been already associated with a positive response to taxanes in preliminary clinical studies.[44] Since Docetaxel acts by binding to the beta-tubulin subunit of the microtubules, resulting in cell-cycle arrest and apoptosis, the presence of an overexpression of tubulin, as we found in our study, could really predict a good response to this drug.

We found that patients responding to CHT have a lower expression of VIME, which has been already correlated with a poor prognosis in other studies.[45] On the other hand, it is known that the expression of VIME in breast cancer cells has been shown to be downstream of several signaling proteins implicated in carcinogenesis[46−48] and its expression might be a requirement for the invasive behavior of the cells.

Finally, the decreased expression of 14−3−3-Z protein, which belongs to a family of protein kinase (PK) inhibitors, and has an antiapoptotic activity, could be another indicator of protection against cancer progression.

Conclusions

In conclusion, the identification of protein clusters associated with response to CHT might be important for predicting the efficacy of specific antineoplastic drugs and for the development of less empiric strategies for choosing the therapy to be prescribed to the single patient. Since clustered proteins identified in this study are mostly secreted by tumor cells, our future work will be the investigation of this proteomic profile in serum. We are aware that there is the need to conduct additional clinical studies on a larger scale to validate these results in the attempt to expand the number of available biomarker assays for early detection and also therapeutic management of cancer, in accordance with the FDA requirements.

Acknowledgment. The authors thank the "Angela Serra" Association for Cancer Research (Modena, Italy) and the Sanofi-Aventis (Milan, Italy) for financial support. A special thank to Dr. Adriano Benedetti and Dr. Daniela Manzini (C.I.G.S., University of Modena and Reggio Emilia) for skilled assistance in protein analysis by ESI-Q-TOF MS.

Supporting Information Available: The 2-DE gels images of all the TIF and NIF samples of patients included in the part of the study concerning the chemotherapy response (Figure 1S) and the magnified spots of proteins differentially expressed after chemotherapy (Figure 2S). The ion spectra for peptide protein identification observed for PTRF is reported in Figure 3S. This material is available free of charge via the Internet at http://pubs.acs.org.

References

(1) Anderson, L.; Seilhamer, J. A comparison of selected mRNA and protein abundances in human liver. *Electrophoresis* **1997**, *18*, 533–7.
(2) Chen, G.; Gharib, T. G.; Wang, H.; Huang, C. C.; Kuick, R.; Thomas, D. G.; Shedden, K. A.; Misek, D. E.; Taylor, J. M.; Giordano, T. J.; Kardia, S. L.; Iannettoni, M. D.; Yee, J.; Hogg, P. J.; Orringer, M. B.; Hanash, S. M.; Beer, D. G. Protein profiles associated with survival in lung adenocarcinoma. *Proc. Natl. Acad. Sci. U.S.A.* **2003**, *100*, 13537–42.
(3) Ginestier, C.; Charafe-Jauffret, E.; Bertucci, F.; Eisinger, F.; Geneix, J.; Bechlian, D.; Conte, N.; Adelaide, J.; Toiron, Y.; Nguyen, C.; Viens, P.; Mozziconacci, M. J.; Houlgatte, R.; Birnbaum, D.; Jacquemier, J. Distinct and complementary information provided by use of tissue and DNA microarrays in the study of breast tumor markers. *Am. J. Pathol.* **2002**, *161*, 1223–33.
(4) Gygi, S. P.; Rochon, Y.; Franza, B. R.; Aebersold, R. Correlation between protein and mRNA abundance in yeast. *Mol. Cell. Biol.* **1999**, *19*, 1720–30.
(5) Nishizuka, S.; Charboneau, L.; Young, L.; Major, S.; Reinhold, W. C.; Waltham, M.; Kouros-Mehr, H.; Bussey, K. J.; Lee, J. K.; Espina, V.; Munson, P. J.; Petricoin, E., III; Liotta, L. A.; Weinstein, J. N. Proteomic profiling of the NCI-60 cancer cell lines using new high-density reverse-phase lysate microarrays. *Proc. Natl. Acad. Sci. U.S.A.* **2003**, *100*, 14229–34.
(6) Tyers, M.; Mann, M. From genomics to proteomics. *Nature* **2003**, *422*, 193–7.
(7) Hondermarck, H.; Vercoutter-Edouart, A. S.; Revillion, F.; Lemoine, J.; el-Yazidi-Belkoura, I.; Nurcombe, V.; Peyrat, J. P. Proteomics of breast cancer for marker discovery and signal pathway profiling. *Proteomics* **2001**, *1*, 1216–32.
(8) Dwek, M. V.; Alaiya, A. A. Proteome analysis enables separate clustering of normal breast, benign breast and breast cancer tissues. *Br. J. Cancer* **2003**, *89*, 305–7.
(9) Wiseman, B. S.; Werb, Z. Stromal effects on mammary gland development and breast cancer. *Science* **2002**, *296*, 1046–9.

(10) Silberstein, G. B. Tumour-stromal interactions. Role of the stroma in mammary development. *Breast Cancer Res* **2001**, *3*, 218–23.
(11) Coussens, L. M.; Werb, Z. Matrix metalloproteinases and the development of cancer. *Chem Biol* **1996**, *3*, 895–904.
(12) Coussens, L. M.; Werb, Z. Inflammatory cells and cancer: think different! *J. Exp. Med.* **2001**, *193*, F23–6.
(13) Fidler, I. J. Angiogenic heterogeneity: regulation of neoplastic angiogenesis by the organ microenvironment. *J. Natl. Cancer Inst.* **2001**, *93*, 1040–1.
(14) Fidler, I. J. Regulation of neoplastic angiogenesis. *J. Natl. Cancer Inst. Monogr.* **2001**, *10*, 4.
(15) Ma, X. J.; Dahiya, S.; Richardson, E.; Erlander, M.; Sgroi, D. C. Gene expression profiling of the tumor microenvironment during breast cancer progression. *Breast Cancer Res.* **2009**, *11*, R7.
(16) Robinson, B. D.; Sica, G. L.; Liu, Y. F.; Rohan, T. E.; Gertler, F. B.; Condeelis, J. S.; Jones, J. G. Tumor microenvironment of metastasis in human breast carcinoma: a potential prognostic marker linked to hematogenous dissemination. *Clin. Cancer Res.* **2009**, *15*, 2433–41.
(17) Celis, J. E.; Gromov, P.; Cabezon, T.; Moreira, J. M.; Ambartsumian, N.; Sandelin, K.; Rank, F.; Gromova, I. Proteomic characterization of the interstitial fluid perfusing the breast tumor microenvironment: a novel resource for biomarker and therapeutic target discovery. *Mol. Cell. Proteomics* **2004**, *3*, 327–44.
(18) Celis, J. E.; Moreira, J. M.; Cabezon, T.; Gromov, P.; Friis, E.; Rank, F.; Gromova, I. Identification of extracellular and intracellular signaling components of the mammary adipose tissue and its interstitial fluid in high risk breast cancer patients: toward dissecting the molecular circuitry of epithelial-adipocyte stromal cell interactions. *Mol. Cell. Proteomics* **2005**, *4*, 492–522.
(19) Gutman, S.; Kessler, L. G. The US Food and Drug Administration perspective on cancer biomarker development. *Nat. Rev. Cancer* **2006**, *6*, 565–71.
(20) Stronach, E. A.; Sellar, G. C.; Blenkiron, C.; Rabiasz, G. J.; Taylor, K. J.; Miller, E. P.; Massie, C. E.; Al-Nafussi, A.; Smyth, J. F.; Porteous, D. J.; Gabra, H. Identification of clinically relevant genes on chromosome 11 in a functional model of ovarian cancer tumor suppression. *Cancer Res.* **2003**, *63*, 8648–55.
(21) Tan, E. Y.; Yan, M.; Campo, L.; Han, C.; Takano, E.; Turley, H.; Candiloro, I.; Pezzella, F.; Gatter, K. C.; Millar, E. K.; O'Toole, S. A.; McNeil, C. M.; Crea, P.; Segara, D.; Sutherland, R. L.; Harris, A. L.; Fox, S. B. The key hypoxia regulated gene CAIX is upregulated in basal-like breast tumours and is associated with resistance to chemotherapy. *Br. J. Cancer* **2009**, *100*, 405–11.
(22) Hussain, S. A.; Ganesan, R.; Reynolds, G.; Gross, L.; Stevens, A.; Pastorek, J.; Murray, P. G.; Perunovic, B.; Anwar, M. S.; Billingham, L.; James, N. D.; Spooner, D.; Poole, C. J.; Rea, D. W.; Palmer, D. H. Hypoxia-regulated carbonic anhydrase IX expression is associated with poor survival in patients with invasive breast cancer. *Br. J. Cancer* **2007**, *96*, 104–9.
(23) Span, P. N.; Bussink, J.; De Mulder, P. H.; Sweep, F. C. Carbonic anhydrase IX expression is more predictive than prognostic in breast cancer. *Br. J. Cancer* **2007**, *96*, 1309, author reply 1310.
(24) Watson, P. H.; Chia, S. K.; Wykoff, C. C.; Han, C.; Leek, R. D.; Sly, W. S.; Gatter, K. C.; Ratcliffe, P.; Harris, A. L. Carbonic anhydrase XII is a marker of good prognosis in invasive breast carcinoma. *Br. J. Cancer* **2003**, *88*, 1065–70.
(25) Parkkila, S.; Rajaniemi, H.; Parkkila, A. K.; Kivela, J.; Waheed, A.; Pastorekova, S.; Pastorek, J.; Sly, W. S. Carbonic anhydrase inhibitor suppresses invasion of renal cancer cells in vitro. *Proc Natl Acad Sci U S A* **2000**, *97*, 2220–4.
(26) Bekku, S.; Mochizuki, H.; Yamamoto, T.; Ueno, H.; Takayama, E.; Tadakuma, T. Expression of carbonic anhydrase I or II and correlation to clinical aspects of colorectal cancer. *Hepatogastroenterology* **2000**, *47*, 998–1001.
(27) Lankat-Buttgereit, B.; Gregel, C.; Knolle, A.; Hasilik, A.; Arnold, R.; Goke, R. Pdcd4 inhibits growth of tumor cells by suppression of carbonic anhydrase type II. *Mol. Cell. Endocrinol.* **2004**, *214*, 149–53.
(28) Chuthapisith, S.; Eremin, J. M.; Eremin, O. Predicting response to neoadjuvant chemotherapy in breast cancer: molecular imaging, systemic biomarkers, and the cancer metabolome. *Oncol. Rep.* **2008**, *20*, 699–703.
(29) Maekawa, M.; Taniguchi, T.; Ishikawa, J.; Sugimura, H.; Sugano, K.; Kanno, T. Promoter hypermethylation in cancer silences LDHB, eliminating lactate dehydrogenase isoenzymes 1−4. *Clin. Chem.* **2003**, *49*, 1518–20.
(30) Maekawa, M.; Inomata, M.; Sasaki, M. S.; Kaneko, A.; Ushiama, M.; Sugano, K.; Takayama, J.; Kanno, T. Electrophoretic variant of a lactate dehydrogenase isoenzyme and selective promoter methylation of the LDHA gene in a human retinoblastoma cell line. *Clin. Chem.* **2002**, *48*, 1938–45.
(31) Chen, Y.; Zhang, H.; Xu, A.; Li, N.; Liu, J.; Liu, C.; Lv, D.; Wu, S.; Huang, L.; Yang, S.; He, D.; Xiao, X. Elevation of serum l-lactate dehydrogenase B correlated with the clinical stage of lung cancer. *Lung Cancer* **2006**, *54*, 95–102.
(32) Lu, H. S.; Yuan, P. M.; Gracy, R. W. Primary structure of human triosephosphate isomerase. *J. Biol. Chem.* **1984**, *259*, 11958–68.
(33) Zhang, D.; Tai, L. K.; Wong, L. L.; Chiu, L. L.; Sethi, S. K.; Koay, E. S. Proteomic study reveals that proteins involved in metabolic and detoxification pathways are highly expressed in HER-2/neu-positive breast cancer. *Mol. Cell. Proteomics* **2005**, *4*, 1686–96.
(34) Lichtenfels, R.; Kellner, R.; Atkins, D.; Bukur, J.; Ackermann, A.; Beck, J.; Brenner, W.; Melchior, S.; Seliger, B. Identification of metabolic enzymes in renal cell carcinoma utilizing PROTEOMEX analyses. *Biochim. Biophys. Acta* **2003**, *1646*, 21–31.
(35) Brown, L. F.; Asch, B.; Harvey, V. S.; Buchinski, B.; Dvorak, H. F. Fibrinogen influx and accumulation of cross-linked fibrin in mouse carcinomas. *Cancer Res.* **1988**, *48*, 1920–5.
(36) Costantini, V.; Zacharski, L. R.; Memoli, V. A.; Kisiel, W.; Kudryk, B. J.; Rousseau, S. M. Fibrinogen deposition without thrombin generation in primary human breast cancer tissue. *Cancer Res.* **1991**, *51*, 349–53.
(37) Wojtukiewicz, M. Z.; Zacharski, L. R.; Memoli, V. A.; Kisiel, W.; Kudryk, B. J.; Rousseau, S. M.; Stump, D. C. Absence of components of coagulation and fibrinolysis pathways in situ in mesothelioma. *Thromb. Res.* **1989**, *55*, 279–84.
(38) Wojtukiewicz, M. Z.; Zacharski, L. R.; Memoli, V. A.; Kisiel, W.; Kudryk, B. J.; Rousseau, S. M.; Stump, D. C. Indirect activation of blood coagulation in colon cancer. *Thromb. Haemostasis* **1989**, *62*, 1062–6.
(39) Costantini, V.; Zacharski, L. R.; Memoli, V. A.; Kisiel, W.; Kudryk, B. J.; Rousseau, S. M.; Stump, D. C. Fibrinogen deposition and macrophage-associated fibrin formation in malignant and non-malignant lymphoid tissue. *J. Lab. Clin. Med.* **1992**, *119*, 124–31.
(40) Rybarczyk, B. J.; Simpson-Haidaris, P. J. Fibrinogen assembly, secretion, and deposition into extracellular matrix by MCF-7 human breast carcinoma cells. *Cancer Res.* **2000**, *60*, 2033–9.
(41) Kavallaris, M.; Kuo, D. Y.; Burkhart, C. A.; Regl, D. L.; Norris, M. D.; Haber, M.; Horwitz, S. B. Taxol-resistant epithelial ovarian tumors are associated with altered expression of specific beta-tubulin isotypes. *J. Clin. Invest.* **1997**, *100*, 1282–93.
(42) Verdier-Pinard, P.; Wang, F.; Martello, L.; Burd, B.; Orr, G. A.; Horwitz, S. B. Analysis of tubulin isotypes and mutations from taxol-resistant cells by combined isoelectrofocusing and mass spectrometry. *Biochemistry* **2003**, *42*, 5349–57.
(43) Galmarini, C. M.; Kamath, K.; Vanier-Viornery, A.; Hervieu, V.; Peiller, E.; Falette, N.; Puisieux, A.; Ann Jordan, M.; Dumontet, C. Drug resistance associated with loss of p53 involves extensive alterations in microtubule composition and dynamics. *Br. J. Cancer* **2003**, *88*, 1793–9.
(44) Galmarini, C. M.; Treilleux, I.; Cardoso, F.; Bernard-Marty, C.; Durbecq, V.; Gancberg, D.; Bissery, M. C.; Paesmans, M.; Larsimont, D.; Piccart, M. J.; Di Leo, A.; Dumontet, C. Class III beta-tubulin isotype predicts response in advanced breast cancer patients randomly treated either with single-agent doxorubicin or docetaxel. *Clin. Cancer Res.* **2008**, *14*, 4511–6.
(45) Thomas, P. A.; Kirschmann, D. A.; Cerhan, J. R.; Folberg, R.; Seftor, E. A.; Sellers, T. A.; Hendrix, M. J. Association between keratin and vimentin expression, malignant phenotype, and survival in postmenopausal breast cancer patients. *Clin. Cancer Res.* **1999**, *5*, 2698–703.
(46) Bindels, S.; Mestdagt, M.; Vandewalle, C.; Jacobs, N.; Volders, L.; Noel, A.; van Roy, F.; Berx, G.; Foidart, J. M.; Gilles, C. Regulation of vimentin by SIP1 in human epithelial breast tumor cells. *Oncogene* **2006**, *25*, 4975–85.
(47) Gilles, C.; Polette, M.; Mestdagt, M.; Nawrocki-Raby, B.; Ruggeri, P.; Birembaut, P.; Foidart, J. M. Transactivation of vimentin by beta-catenin in human breast cancer cells. *Cancer Res.* **2003**, *63*, 2658–64.
(48) Minard, M. E.; Ellis, L. M.; Gallick, G. E. Tiam1 regulates cell adhesion, migration and apoptosis in colon tumor cells. *Clin. Exp. Metastasis* **2006**, *23*, 301–13.

PR900239H